ERC STARTING GRANT

Probing the Micro-Nano Transition (MINATRAN): Theoretical and Experimental Foundations, Simulations and -Applications [1.3 Million Euros]
2008-2013

With PhD advisors Profs De Hosson and Willis.

Dr. Potocnik
European Commissioner for Research

0. A GLIMPSE THROUGH GRADIENT PLASTICITY

■ Motivation from Averaging

- ***Self - Consistent Approximation***

- Simple Shear

$$\tau = \bar{\tau} - \beta \Delta\gamma$$

$$\bar{\tau} = \kappa(\bar{\gamma}) \,,\; \beta = \alpha\mu\{1 - 2S_{1212}\} \quad , \quad \Delta\gamma = \gamma - \bar{\gamma}$$

$$\bar{\gamma} = \frac{1}{V}\int_V \gamma(\boldsymbol{x}+\boldsymbol{r})dV \quad , \qquad V = \frac{4}{3}\pi R^3 \quad \Rightarrow$$

$$\gamma(\boldsymbol{x}+\boldsymbol{r}) = \gamma(\boldsymbol{x}) + \nabla\gamma\cdot\boldsymbol{r} + \frac{1}{2!}\nabla^{(2)}\gamma\cdot\boldsymbol{r}\otimes\boldsymbol{r} + \ldots; \int_V \nabla^{2n+1}\gamma\cdot\boldsymbol{r}^{2n+1}dV = 0$$

$$\bar{\gamma} \approx \gamma + \frac{R^2}{10}\nabla^2\gamma \quad ,$$

$$\tau = \kappa(\gamma) - \frac{R^2}{10}(\beta + h)\nabla^2\gamma \quad ; \qquad \begin{cases} R = d/2 \\ \beta = \alpha\mu\dfrac{7-5\nu}{15(1-\nu)} \\ h = d\bar{\tau}/d\bar{\gamma} \end{cases}$$

$$\therefore \quad c = \frac{R^2}{10}(\beta + h) \qquad \Rightarrow \qquad c = Cd^2$$

Plastic Boundary Layers

- ***Fleck/Van Der Giessen/Needleman (2000)***

Discrete Dislocations (DD)

$u_1 = U(t), u_2 = 0$

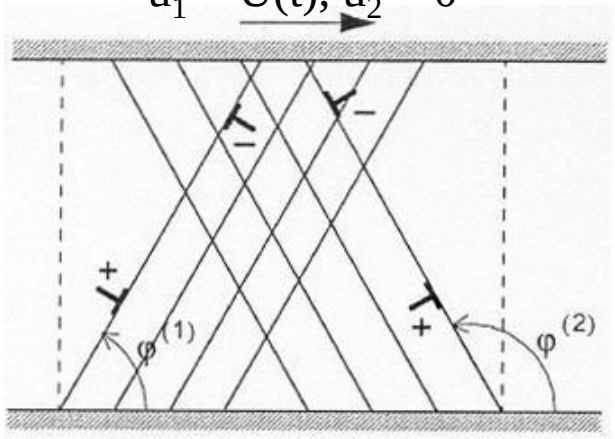

$u_1 = 0, u_2 = 0$

Fleck-Hutchinson (F-H)

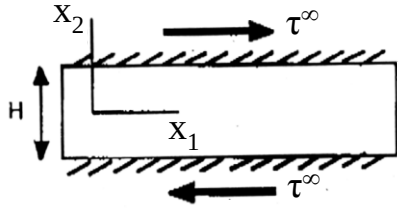

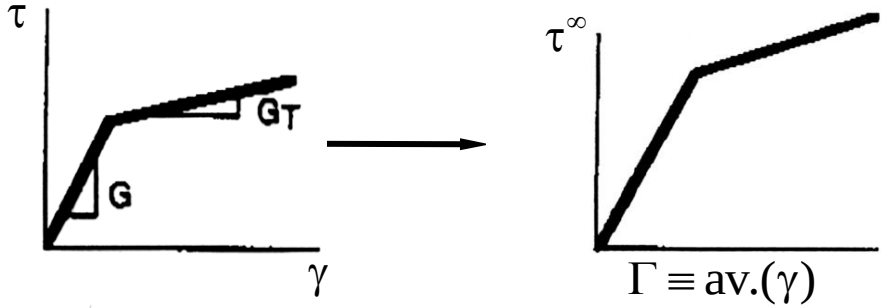

- ***Aifantis (1984) / Gurtin (2000)***

$$\tau = \tau_0 + G_T\gamma - G_T\ell^2\nabla^2\gamma = \tau^\infty \;\Rightarrow\; \gamma = \frac{\tau^\infty}{G} + \frac{\tau^\infty - \tau_0}{G_T}\left[1 - \frac{\cosh(x_2/\ell)}{\cosh(H/\ell)}\right]$$

$$\Gamma = \frac{1}{H}\int_{-H/2}^{H/2}\gamma(x_2)dx_2 = \frac{\tau^\infty}{G} + \frac{\tau^\infty - \tau_0}{G_T}\left(1 - \frac{2\ell}{H}\tanh\frac{H}{2\ell}\right)$$

- ***Plastic Strain Profiles / Size Effects***

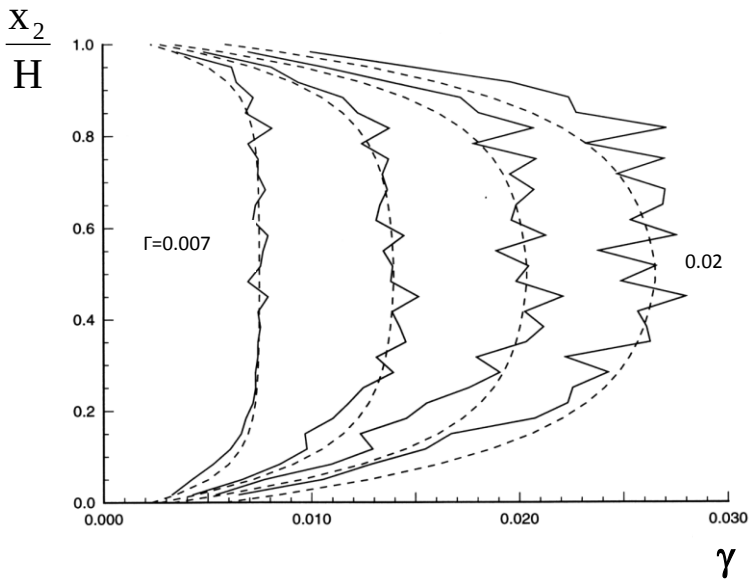

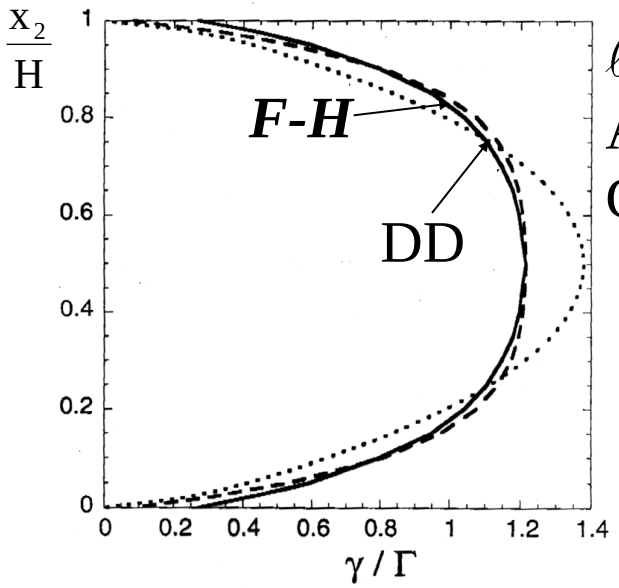

$\ell = 0.1\mu m$
Aifantis/
Gurtin

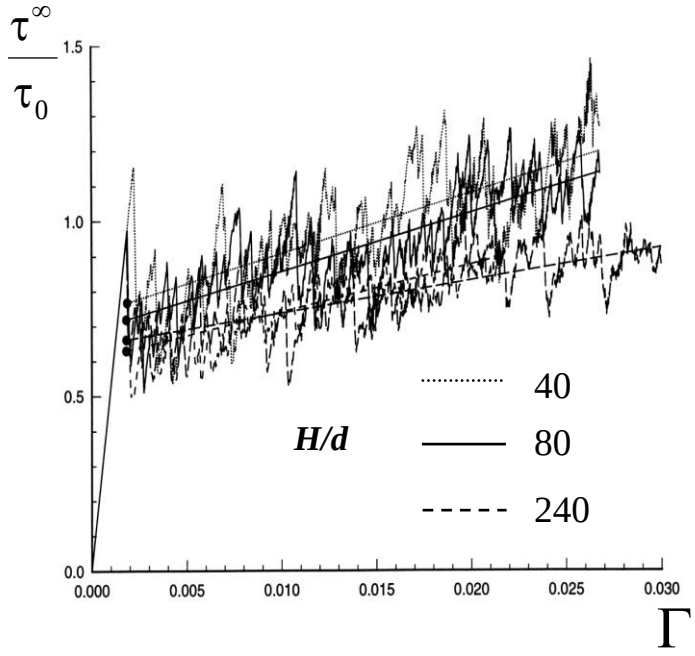

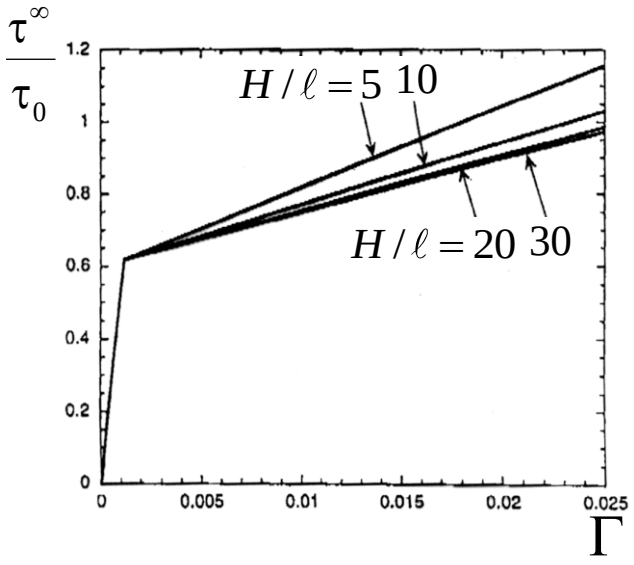

Size Effects in Tension/Compression

- ***Lack of Macroscopic Gradients in Tension***

a) Steel cylindrical macro-bars

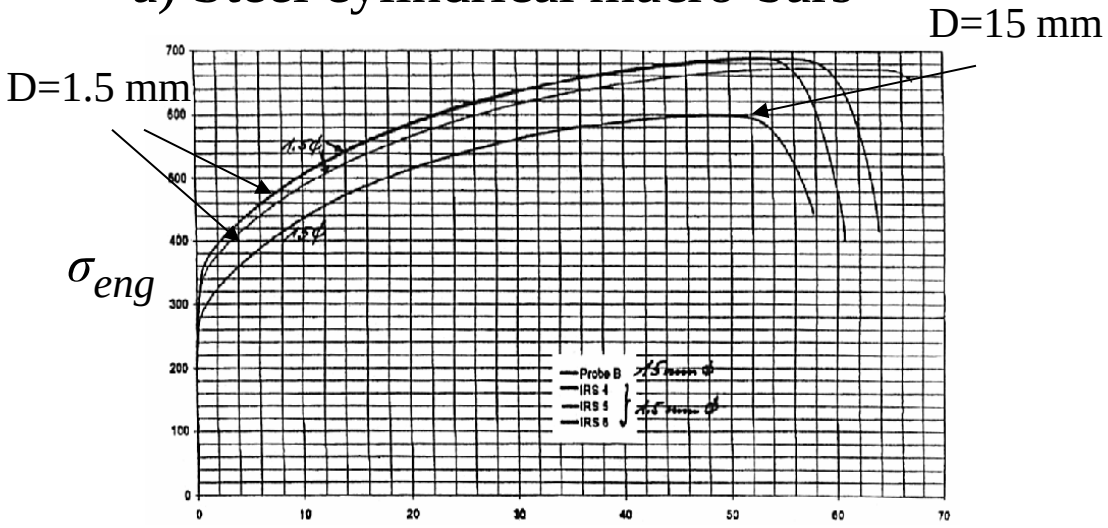

Data from ECA et al 1998

b) Ag micro-wires

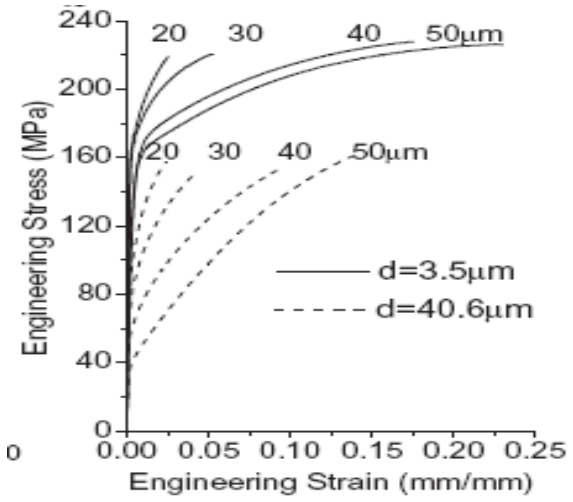

Data from Ngan 2011

Size effect modeling? → Gradient Internal Variable "α"

$$\sigma = \kappa(\varepsilon) + \lambda(\bar{\alpha}) \quad ; \quad \bar{\alpha} = \frac{1}{\upsilon}\int_{\upsilon} \alpha d\upsilon \ , \ \dot{\alpha} = D\nabla^2\alpha + \Lambda\varepsilon^q - M\alpha$$

i.e.

"σ"depends on ε and an averaged internal variable "$\bar{\alpha}$" whose microscopic counterpart "α" evolves inhomogeneously: ∇^2 transport term

- ***Adiabatic Elimination of "α"*** $(\dot{\alpha} \sim 0)$

  - *Radial symmetry* $\alpha = \alpha(r)$

$$\Rightarrow \alpha(r) = AK_0\left(r/\sqrt{c}\right) + BI_0\left(r/\sqrt{c}\right) + \lambda\varepsilon^q \qquad \begin{cases} c \equiv D/M \\ \lambda \equiv \Lambda/M \end{cases}$$

BC's : $\alpha(r)$ finite $\quad \forall\, r > 0 \Rightarrow A \equiv 0$

$$\left.\frac{\partial \alpha}{\partial r}\right|_{r=R} = \frac{\alpha_c}{\sqrt{c}} = \frac{\lambda\varepsilon^q}{\sqrt{c}} \qquad \ldots \text{ zero flux of } \alpha \text{ at } r = 0$$

- *Assume* : $\kappa(\varepsilon) = Y + k_0\varepsilon^n$ (*); $\quad \lambda(\bar{\alpha}) = k_0^*\bar{\alpha}^m$ … Ludwig type

$$\therefore \quad \sigma = Y + k_0\varepsilon^n + k_0^*\left[\lambda\varepsilon\right]^{qm}\left[1 + 2\beta e^{\varepsilon/2}\right]^m \qquad (**)$$

(**) Interprets the size effects in tension of previous slide

- *Note* : Grain size dependence can be introduced in (*), e.g. according to H-P relation, in order to capture intrinsic (d) and extrinsic (D) size effects simultaneously

- ***Size Effects on Tensile Strength of Mg Microwires***

$$k_0 = 40\ \text{MPa};\quad m = n = 0.6;\quad q = 1;\quad \ell = 3.5\ \mu\text{m}$$

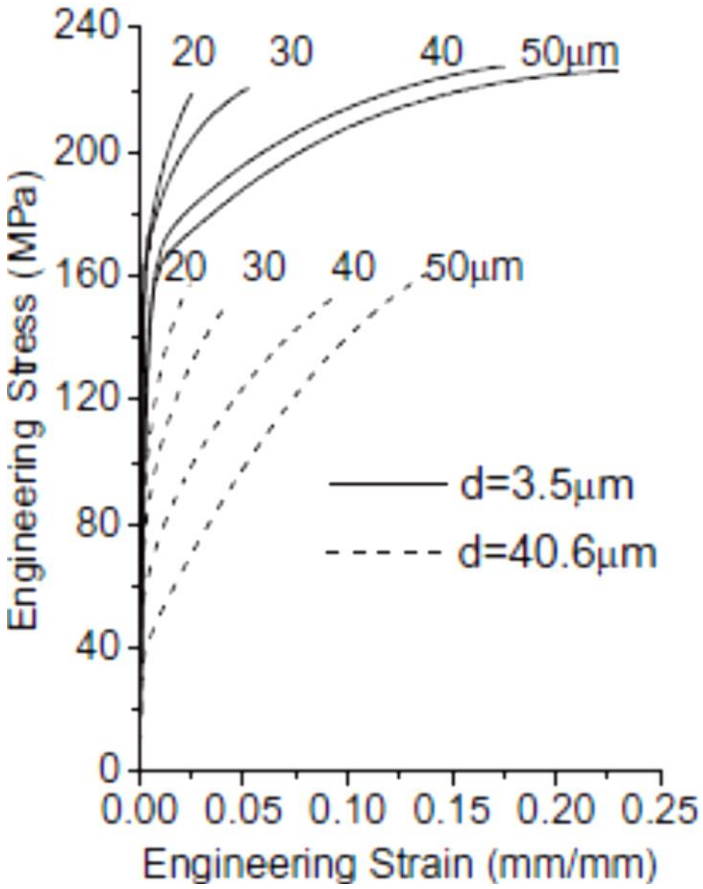

(Chen & Ngan, 2011)

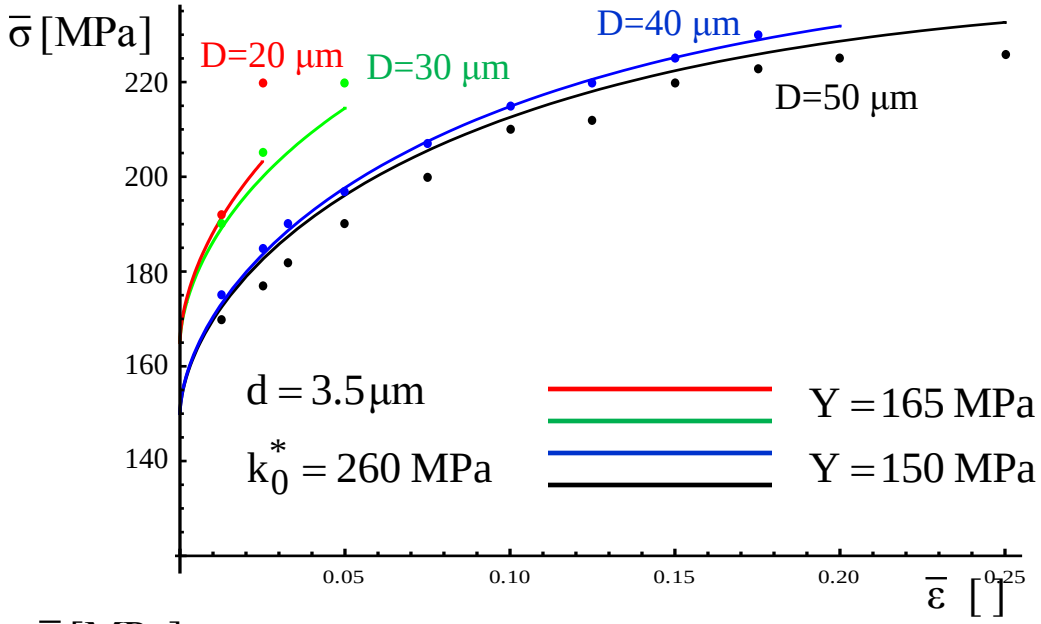

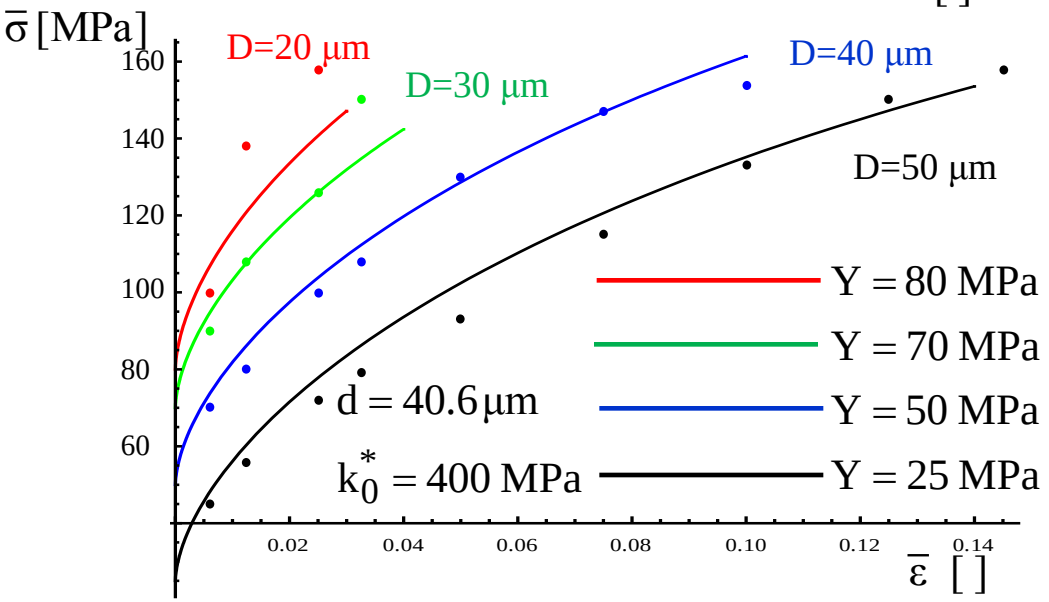

- ***Modified H-P Relation: Application to Ag Nanowires***

$$Y = Y_0 + \frac{k_Y}{\sqrt{d}} + \frac{k_Y^*}{d}$$

$D/d > 3$: $k_Y = 300\ \text{MPa}\sqrt{\mu\text{m}}$ (H-P)

$D/d < 3$: $k_Y = 100\ \text{MPa}\sqrt{\mu\text{m}}$; $k_Y^* = 210\ \text{N/m}$ (Modified H-P)

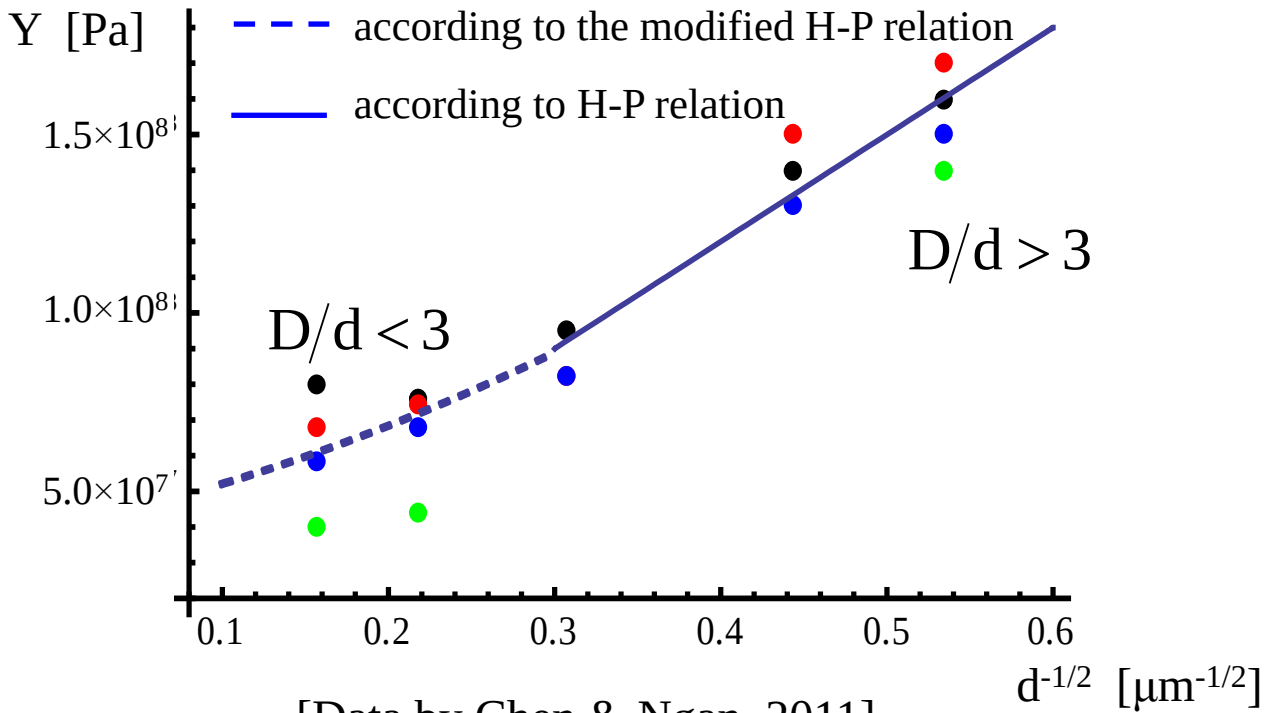

[Data by Chen & Ngan, 2011]

- ***Size Effects in Yield of Micropillars***

$$\sigma = Y + k\varepsilon^{n} + k^{*}\varepsilon\left[1 + 2\beta e^{\varepsilon/2}\right]^{m};\ \beta = \frac{2\ell}{D} \rightarrow \sigma = \frac{Y + k\ln(1+\bar{\varepsilon})^{n} + k^{*}\ln(1+\bar{\varepsilon})\left(1 + 4\frac{\ell}{D}(1+\bar{\varepsilon})\right)^{m}}{(1+\bar{\varepsilon})}$$

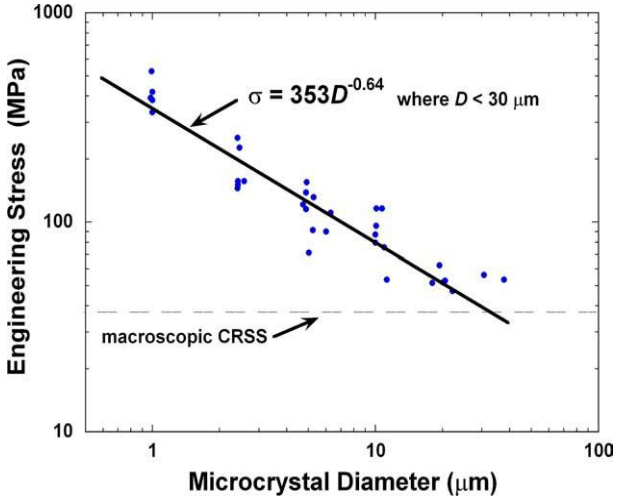

(Dimiduk et al, 2005)

σ_Y [MPa]

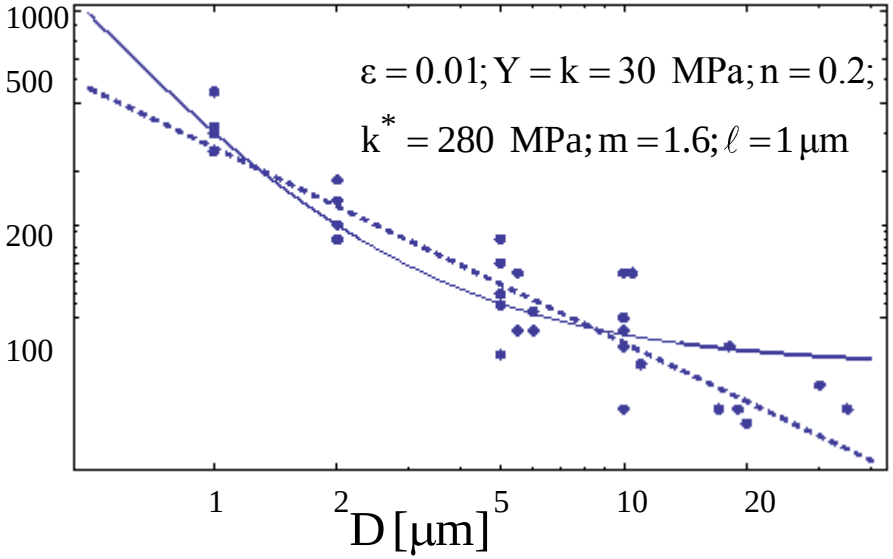

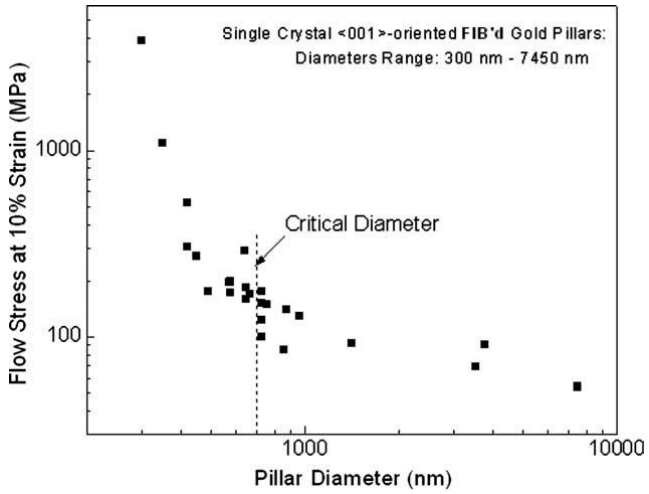

(Greer et al, 2005)

σ_Y [MPa]

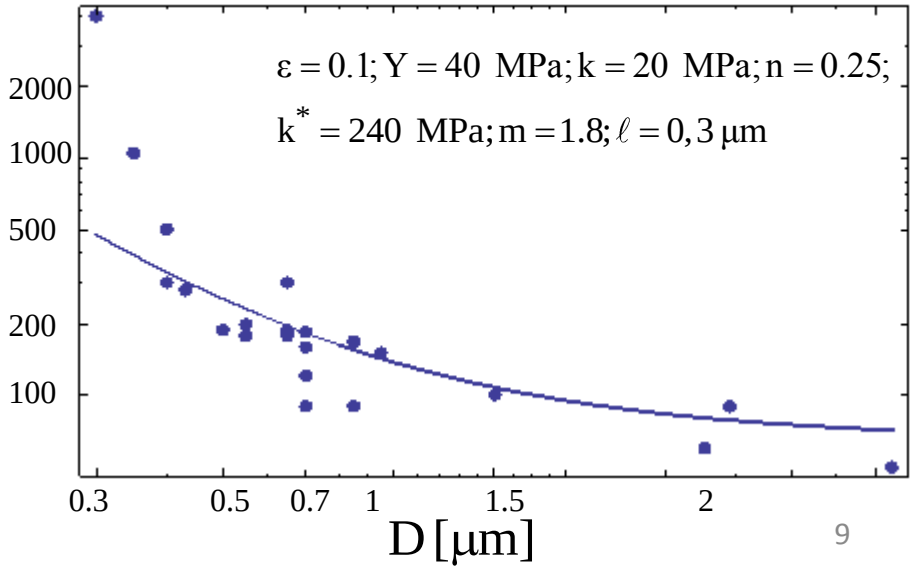

I. MECHANICAL RESPONSE OF MICROPILLARS

Aifantis-Willis Strain Gradient Model

Energy Function

$$\Psi\left(\varepsilon_{ij},\varepsilon_{ij}^{\mathrm{p}}\right)=\int_{\Omega}U\left(\varepsilon_{ij},\varepsilon_{ij}^{\mathrm{p}},\varepsilon_{ij,k}^{\mathrm{p}}\right)\mathrm{d}\Omega-\int_{\partial\Omega_i^t}\left(t_i^0\delta u_i\right)\mathrm{dS}-\int_{\partial\Omega_{ij}^m}\left(m_{ij}^0\delta\varepsilon_{ij}^{\mathrm{p}}\right)\mathrm{dS}+\int_{\Gamma}\Phi(\varepsilon_{ij}^{\mathrm{p}})\mathrm{d}\Gamma$$

Traction | Hyper traction | Interface energy

Elastoplastic Gradient Potential

$$U(\varepsilon_{ij},\varepsilon_{ij}^{\mathrm{p}},\varepsilon_{ij,k}^{\mathrm{p}})=\frac{1}{2}(\varepsilon_{ij}-\varepsilon_{ij}^{\mathrm{p}})L_{ijkl}(\varepsilon_{kl}-\varepsilon_{kl}^{\mathrm{p}})+V(\varepsilon_{ij}^{\mathrm{p}},\varepsilon_{ij,k}^{\mathrm{p}})$$

Conjugate Variables

Cauchy stress $\sigma_{ij}=\dfrac{\partial U}{\partial\varepsilon_{ij}}=L_{ijkl}\left(\varepsilon_{kl}-\varepsilon_{kl}^{\mathrm{p}}\right)$

Back stress $s_{ij}=\dfrac{\partial U}{\partial\varepsilon_{ij}^{\mathrm{p}}}=-L_{ijkl}\left(\varepsilon_{kl}-\varepsilon_{kl}^{\mathrm{p}}\right)+\dfrac{\partial V}{\partial\varepsilon_{ij}^{\mathrm{p}}}=-\sigma_{ij}+\dfrac{\partial V}{\partial\varepsilon_{ij}^{\mathrm{p}}}$

Hyper stress $\tau_{ijk}=\dfrac{\partial U}{\partial\varepsilon_{ij,k}^{\mathrm{p}}}=\dfrac{\partial V}{\partial\varepsilon_{ij,k}^{\mathrm{p}}}$

Variational Principle

$$\delta\Psi^{\mathrm{p}}\left(\varepsilon_{ij},\varepsilon_{ij}^{\mathrm{p}}\right)=\int_{\Omega}\left(\sigma_{ij}\delta\varepsilon_{ij}+s_{ij}\delta\varepsilon_{ij}^{\mathrm{p}}+\tau_{ijk}\delta\varepsilon_{ij,k}^{\mathrm{p}}\right)\mathrm{d}\Omega-\int_{\partial\Omega_i^t}\left(t_i^0\delta u_i\right)\mathrm{dS}-\int_{\partial\Omega_{ij}^m}\left(m_{ij}^0\delta\varepsilon_{ij}^{\mathrm{p}}\right)\mathrm{dS}+\int_{\Gamma}\Phi(\varepsilon_{ij}^{\mathrm{p}})\mathrm{d}\Gamma=0$$

Cauchy stress | Back stress | Hyper stress | Traction | Hyper traction | Interface energy

$$\sigma_{ij,j}=0 \quad \text{in } \Omega$$
$$s_{ij}=\tau_{ijk,k} \quad \text{in } \Omega$$

Equilibrium equations

$$\sigma_{ij}n_j=t_i^0 \quad \text{on } \partial\Omega_i^t$$
$$\tau_{ijk}n_k=m_{ij}^0 \quad \text{on } \partial\Omega_{ij}^m$$

Natural boundary conditions

$$u_i=\bar{u}_i \quad \text{on } \partial\Omega_i^u$$
$$\varepsilon_{ij}^{\mathrm{p}}=\bar{\varepsilon}_{ij}^{\mathrm{p}} \quad \text{on } \partial\Omega_{ij}^{\varepsilon}$$

Essential boundary conditions

$$\left[\sigma_{ij}n_j\right]=0, \quad \text{on } \Gamma$$
$$\left[\tau_{ijk}n_k\right]=\Phi', \quad \text{on } \Gamma$$

Interface conditions

Solution of Aifantis-Willis Model in 1D

$$\sigma_{,x} = 0 \quad \text{in } \Omega$$
$$s = \tau_{,x} \quad \text{in } \Omega$$

Equilibrium equations

$$\sigma = t^0 \quad \text{on } \partial\Omega^t$$
$$\tau = m^0 \quad \text{on } \partial\Omega^m$$

Natural boundary conditions

$$u = \bar{u} \quad \text{on } \partial\Omega^u$$
$$\varepsilon^{\mathrm{p}} = \bar{\varepsilon}^{\mathrm{p}} \quad \text{on } \partial\Omega^{\varepsilon}$$

Essential boundary conditions

$$\sigma\left(\Gamma^+\right) = \sigma\left(\Gamma^-\right)$$
$$\left[\tau\right] = \tau\left(\Gamma^+\right) - \tau\left(\Gamma^-\right) = \Phi'\big|_{\Gamma}$$

Interface conditions

To solve the boundary value problem, we need further to define the gradient plastic potential V and interface energy F for specific problems

Plastic Potential

$$V\left(\varepsilon^{\mathrm{p}}, \varepsilon^{\mathrm{p}}_{,x}\right) = \sigma^{\mathrm{ys}}\left|\varepsilon^{\mathrm{p}}\right| + \frac{1}{2}\beta\left(\varepsilon^{\mathrm{p}}\right)^2 + \frac{1}{2}\beta\ell^2\left(\varepsilon^{\mathrm{p}}_{,x}\right)^2$$

Yield stress | SSD hardening | GND hardening

Interface Energy

$$\Phi\left(\varepsilon^{\mathrm{p}}_{\Gamma}\right) = \gamma\left|\varepsilon^{\mathrm{p}}_{\Gamma}\right| + \frac{1}{2}\alpha\left(\varepsilon^{\mathrm{p}}_{\Gamma}\right)^2$$

Interface yielding | Interface hardening

Application of Aifantis-Willis Model

(2) Analytical Expression for $\sigma_{gb}^{ys} = \bar{\sigma}_c$, characterizing the onset of dislocation transfer across interfaces; also fitting well the experimental data. [1] K.E. Aifantis, A.H.W. Ngan, *Mater Sci Eng A* **459**, 251 (2007). [2] K. E. Aifantis, W. A. Soer, J.T.M. De Hosson, J. R. Willis, *Acta Mater* **54**, 5077 (2006).

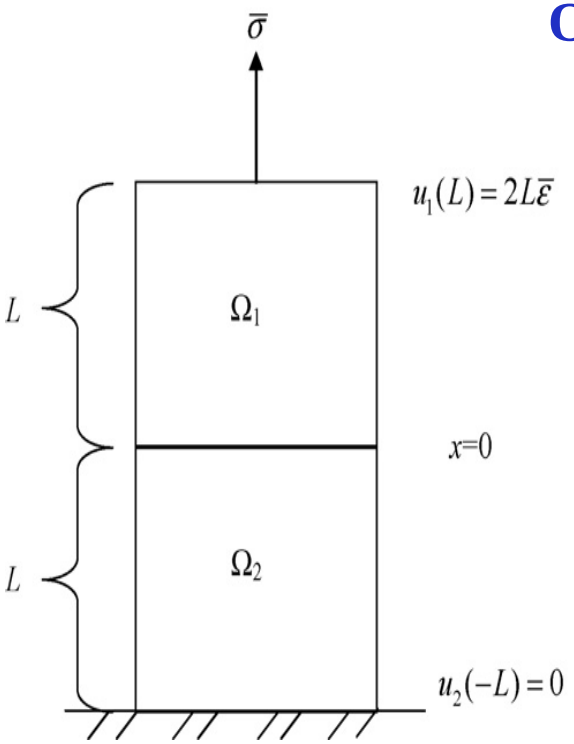

Overall Stress – Strain Response

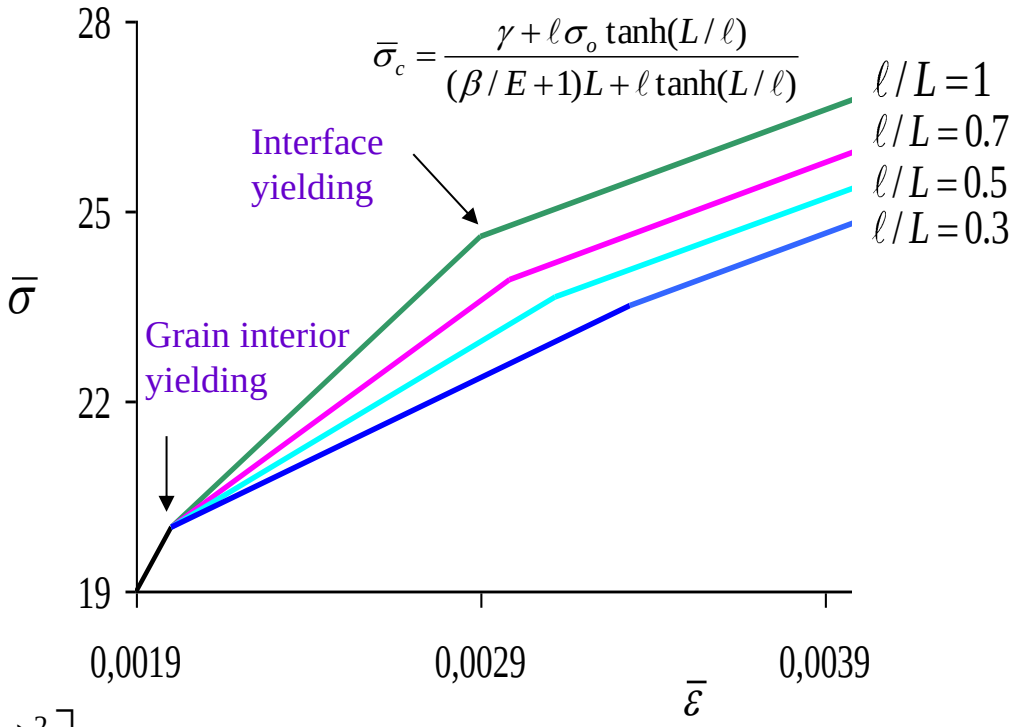

$$V_i(\varepsilon_i^p, \varepsilon_{i,x}^p) = \sigma_0 \left|\varepsilon_i^p\right| + \frac{1}{2}\beta\left[(\varepsilon_i^p)^2 + \ell^2(\varepsilon_{i,x}^p)^2\right]$$

$$\Phi\left(\varepsilon_\Gamma^p\right) = \gamma\left|\varepsilon_\Gamma^p\right|$$

- New yield mechanism: Grain boundary yielding $\bar{\sigma}_c$
- New size effect: Due to both ℓ and g

Nanoindentation experiment near Fe–2.2% Si grain boundary

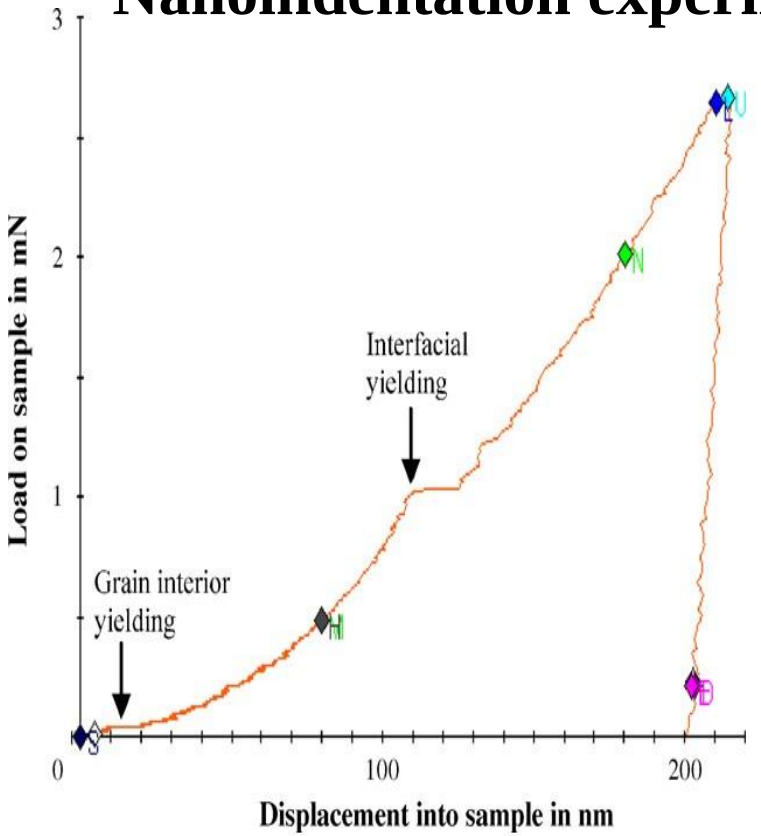

Indent	Distance of tip to boundary at onset of burst (nm)	CSM hardness at onset of burst (GPa)	Interfacial yield stress (GPa)
1	210	3.20	1.067
2	131	3.70	1.23
3	335	3.17	1.057
4	106	4.25	1.42

$$\sigma_c = \frac{\gamma}{2L}\coth\left(\frac{L}{\ell}\right)$$

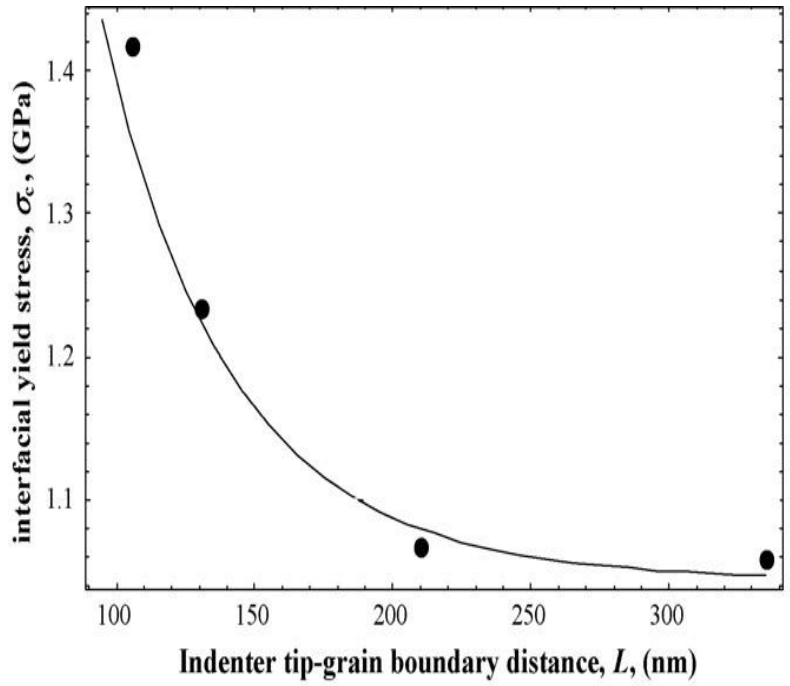

$$V_i(\varepsilon_i^{\mathrm{p}}, \varepsilon_{i,x}^{\mathrm{p}}) = \frac{1}{2}\beta\left[(\varepsilon_i^{\mathrm{p}})^2 + \ell^2(\varepsilon_{i,x}^{\mathrm{p}})^2\right]$$

$$\Phi\left(\varepsilon_\Gamma^{\mathrm{p}}\right) = \gamma\left|\varepsilon_\Gamma^{\mathrm{p}}\right|$$

(3) Trilinear response of bicrystal. X. Zhang, K.E. Aifantis, A. Ngan, *forthcoming*.

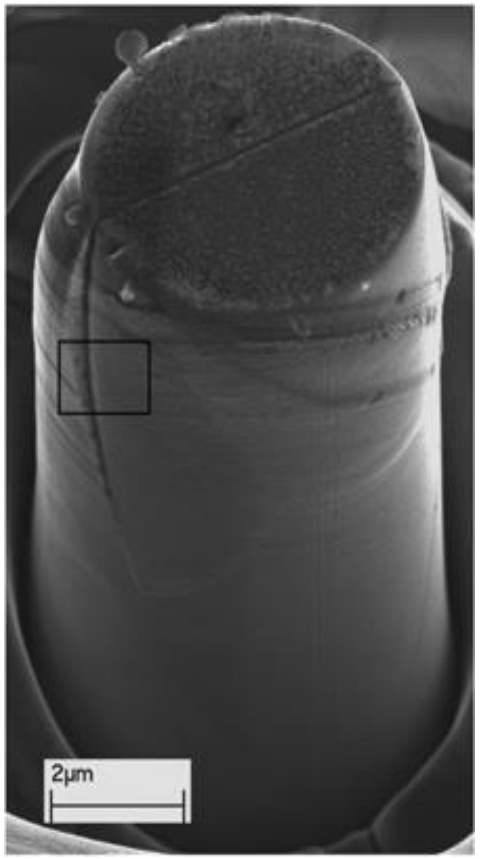

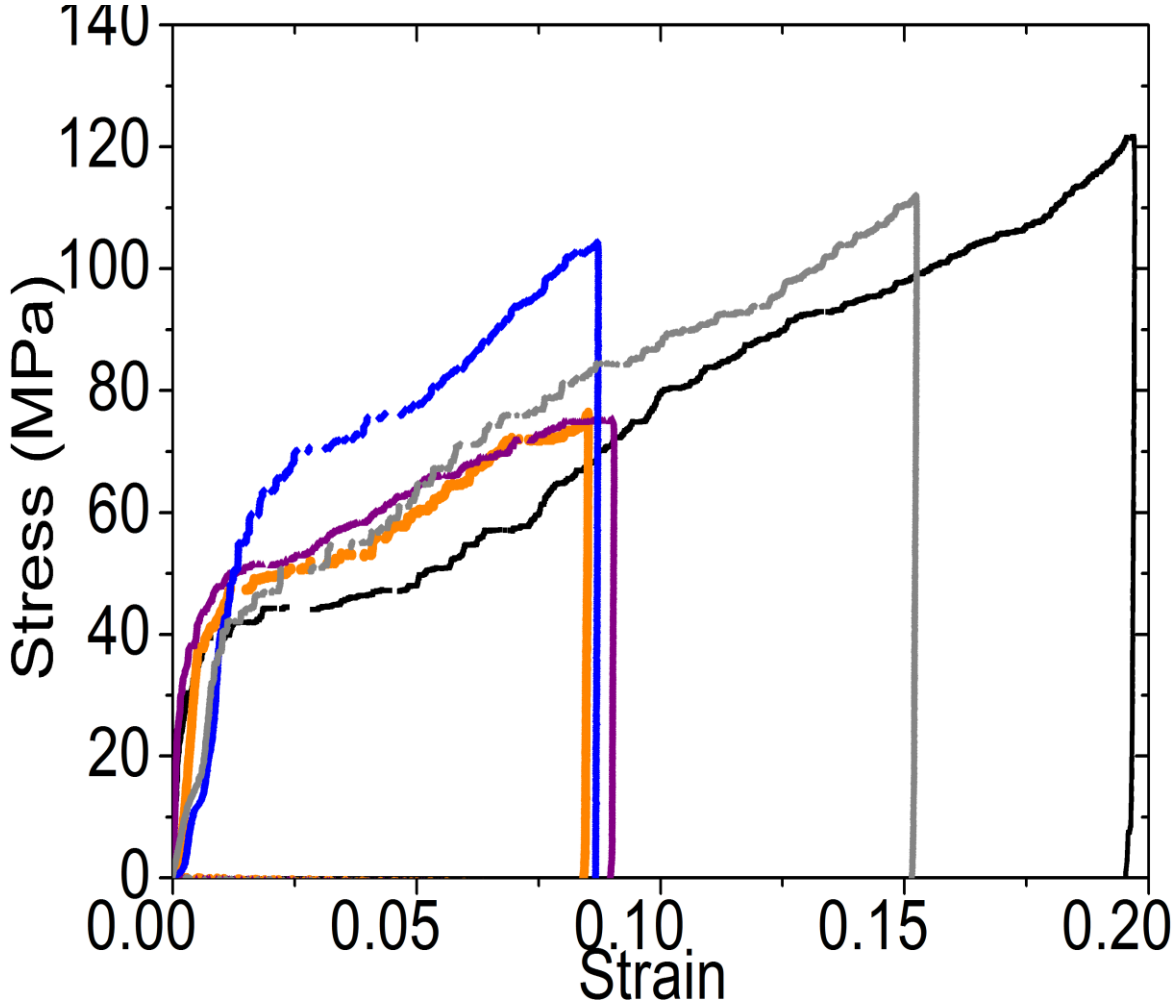

Stage 1: Elastic

$$\bar{\sigma} = E\bar{\varepsilon}$$

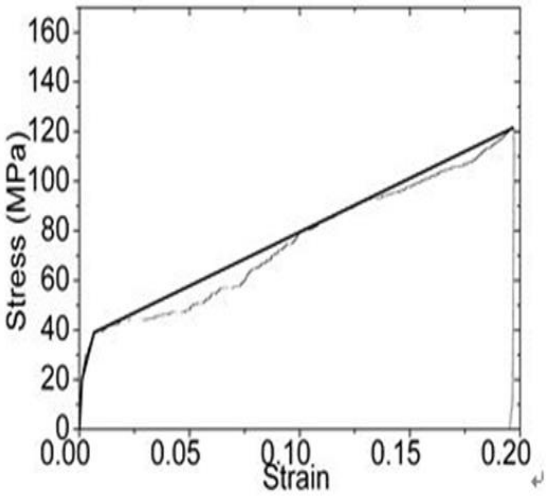

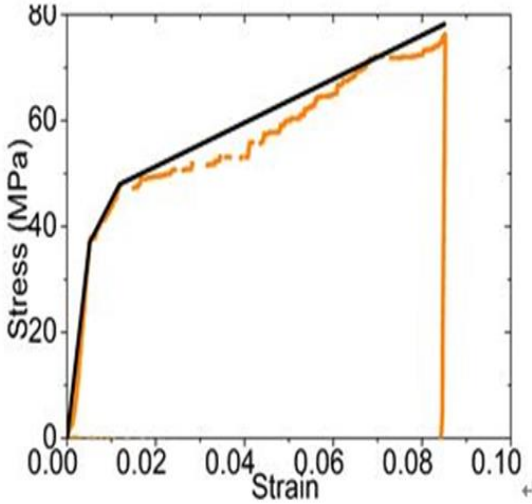

Stage 2: Grain yielding

$$\bar{\sigma} = \sigma_{\mathrm{g}}^{\mathrm{ys}} + \left[\frac{1}{E} + \frac{1}{\beta}\left(1 - \frac{\ell}{L}\mathrm{Tanh}\left(\frac{L}{\ell}\right)\right)\right]^{-1}\left(\bar{\varepsilon} - \frac{\sigma_{\mathrm{g}}^{\mathrm{ys}}}{E}\right)$$

Stage 3: Grain boundary yielding

$$\bar{\sigma} = \frac{E\left[2L\left(\sigma_{\mathrm{g}}^{\mathrm{ys}} + \beta\bar{\varepsilon}\right) + \gamma\right]}{2\left(\beta + E\right)L}$$

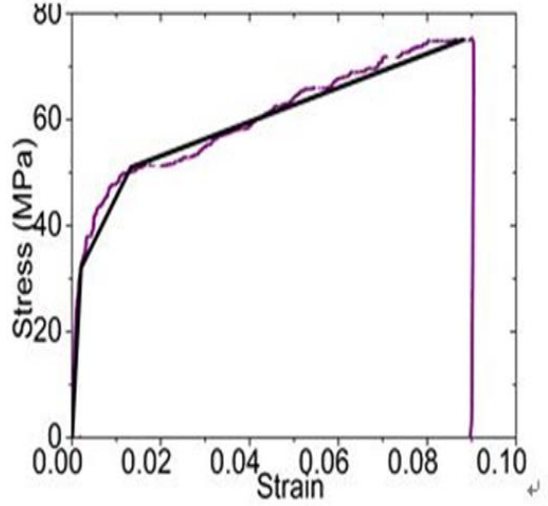

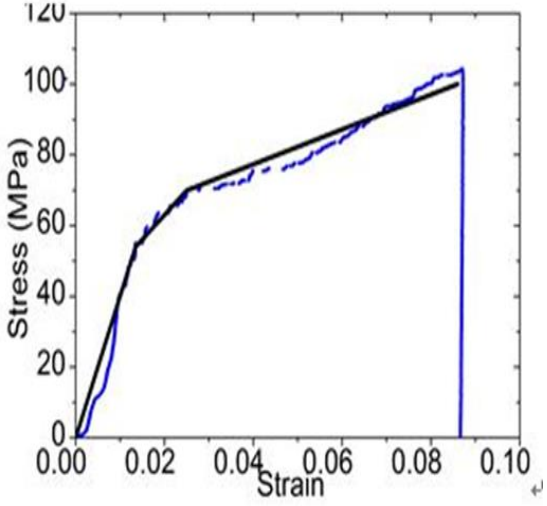

(4) HP and Inverse HP Effect. [1] X. Zhang, K.E. Aifantis, *J. Mater. Res.***26**, 1399 (2011), [2] K.E. Aifantis, A.A. Konstantinidis, *Mater. Sci. Eng. A* **503**, 198 (2009).

$$\tau_{\mathrm{gb}}\left(L_{\mathrm{gb}}\right)-\tau_{\mathrm{gb}}\left(-L_{\mathrm{gb}}\right)=\gamma_{\mathrm{gb}}\Rightarrow\bar{\sigma}=\sigma_0+\frac{k}{\sqrt{d}}+\frac{\gamma_{\mathrm{gb}}}{2ad}$$

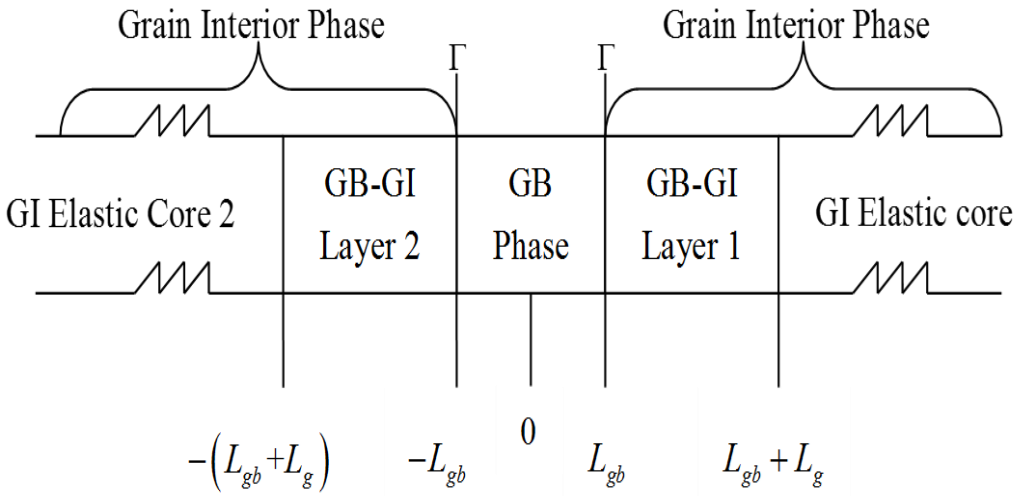

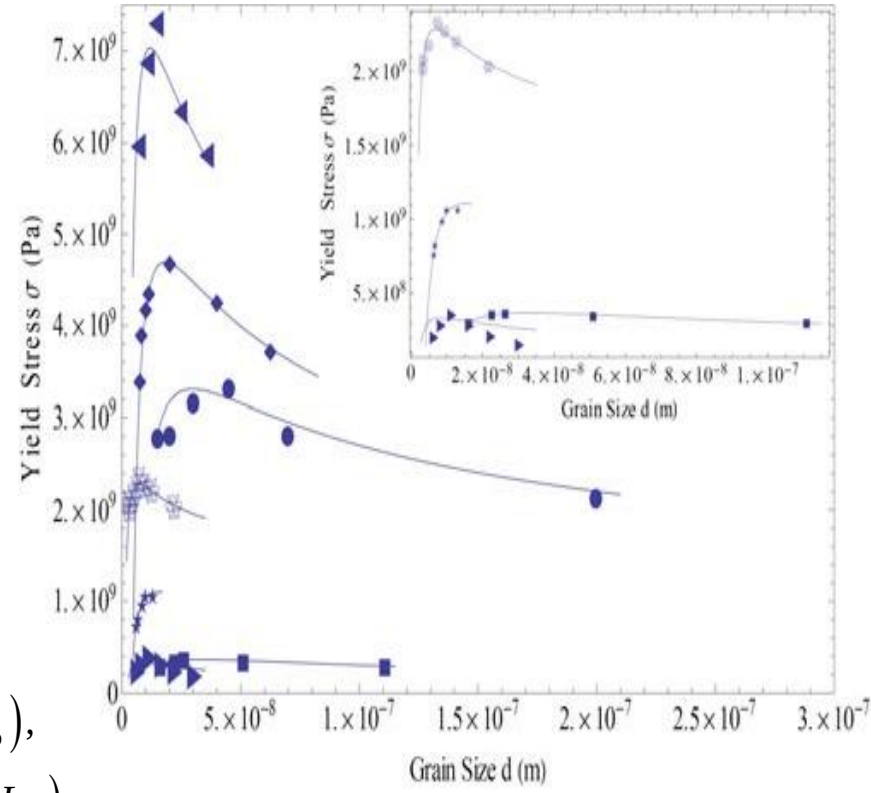

$$\varepsilon_{\mathrm{g1}}^{\mathrm{p}}\left(L_{\mathrm{gb}}+L_{\mathrm{g}}\right)=0,\qquad \varepsilon_{\mathrm{g1}}^{\mathrm{p}}\left(L_{\mathrm{gb}}\right)=\varepsilon_{\mathrm{gb}}^{\mathrm{p}}\left(L_{\mathrm{gb}}\right),\qquad \tau_{\mathrm{g1}}\left(L_{\mathrm{gb}}\right)=\tau_{\mathrm{gb}}\left(L_{\mathrm{gb}}\right),$$

$$\varepsilon_{\mathrm{g2}}^{\mathrm{p}}\left(-L_{\mathrm{gb}}-L_{\mathrm{g}}\right)=0,\qquad \varepsilon_{\mathrm{g2}}^{\mathrm{p}}\left(-L_{\mathrm{gb}}\right)=\varepsilon_{\mathrm{gb}}^{\mathrm{p}}\left(-L_{\mathrm{gb}}\right),\qquad \tau_{\mathrm{g2}}\left(-L_{\mathrm{gb}}\right)=\tau_{\mathrm{gb}}\left(-L_{\mathrm{gb}}\right).$$

Compression Behavior of Micropillars

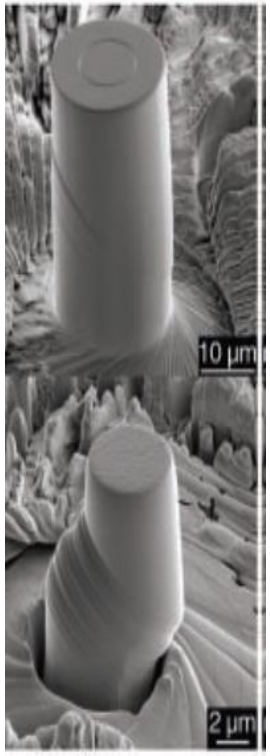

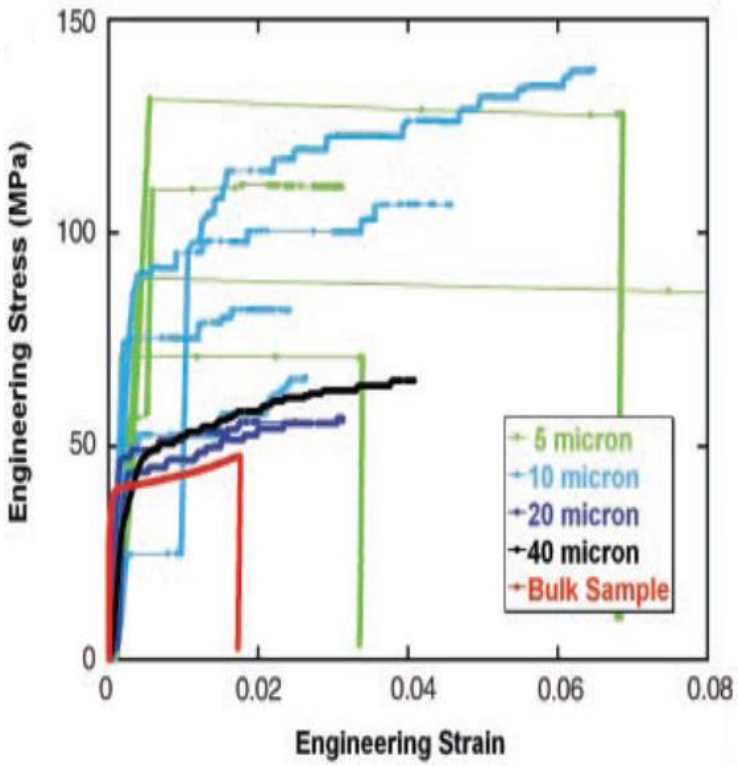

(Uchic et al., Science, 2004,305:986)

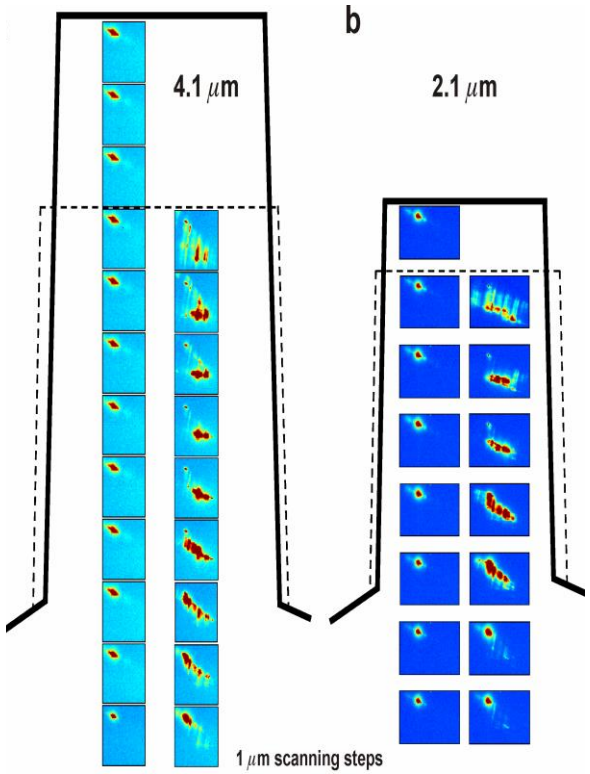

(Maass et al, Physical Review Letters, 2007. 99(14))

- Yield stress and flow stress increase with the decrease of the pillar size
- Strain bursts in the stress-strain curve
- Stochasticity: pillars of same diameter---->different response
- In-situ synchrotron microdiffraction experiments indicating significant dislocation evolution during compression

Strain Gradient Multilayer Model

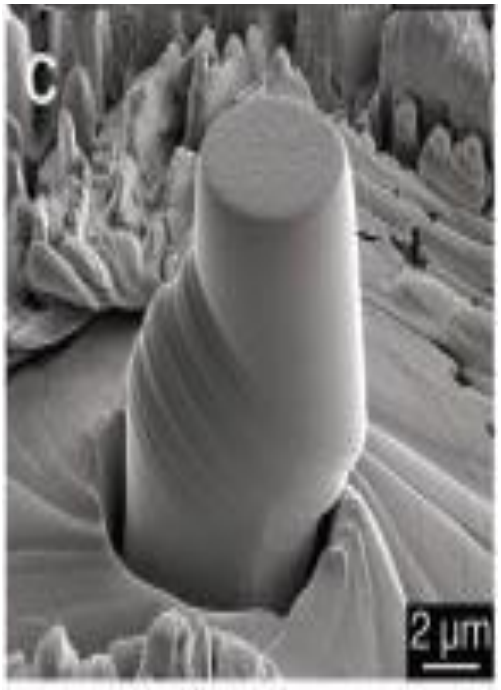

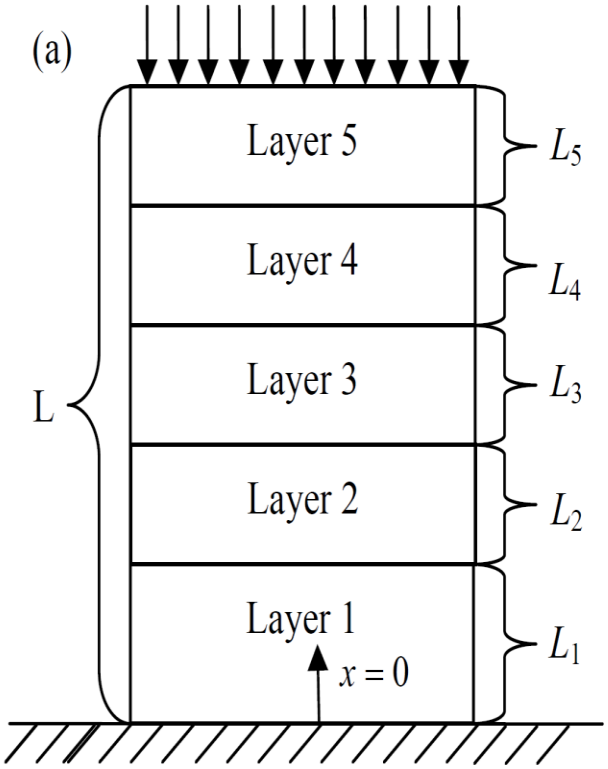

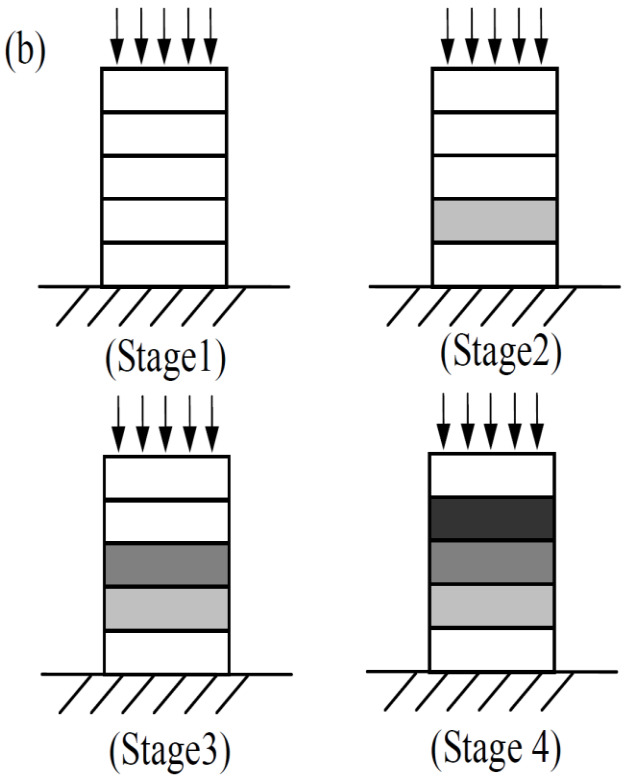

[Stochastic Properties]

The pillar is therefore divided into elastic and plastic zones. Each slip zone is identified with a thin layer that is characterized by a different yield stress, elastic modulus and hardening modulus from the adjacent layers.

Stress-Strain Response

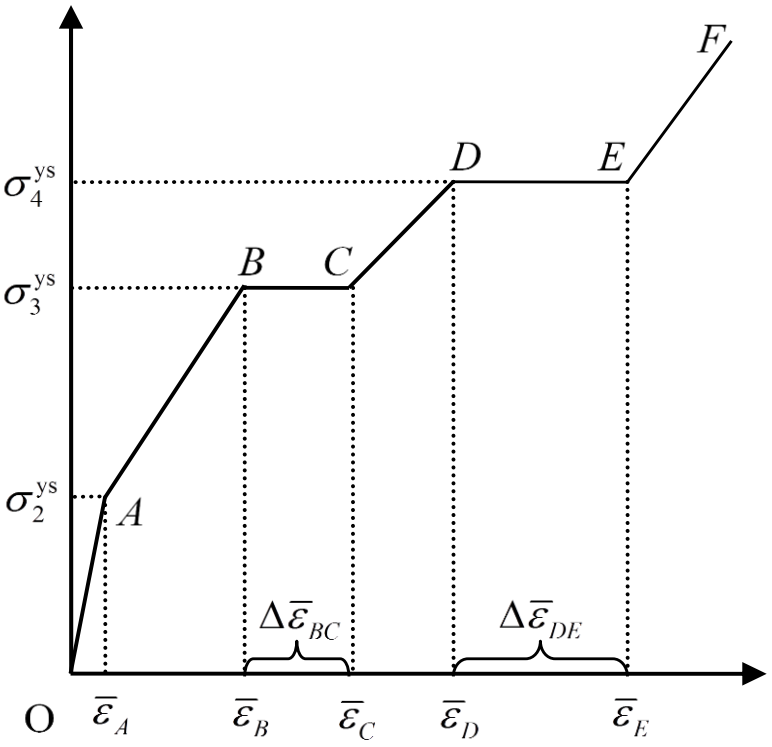

(a)Stress-strain curve of 5 layers model

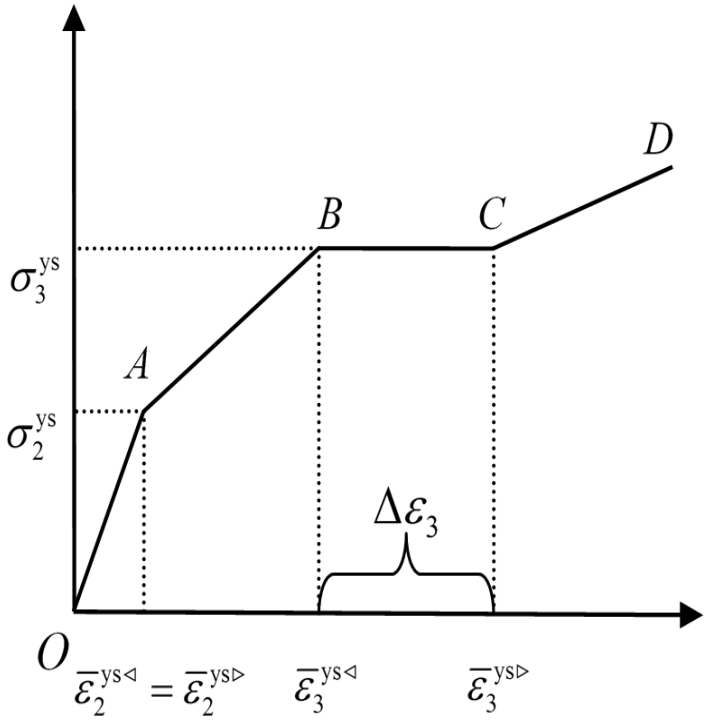

(b) Stress-strain curve of 4 layers model

- **The transition from discontinuity to continuity of the hyper stress across the internal boundary between two neighboring layers results in a strain burst.**

- **More strain bursts would appear by increasing the number of slip layers; additional slip layers correspond to more strain bursts.**

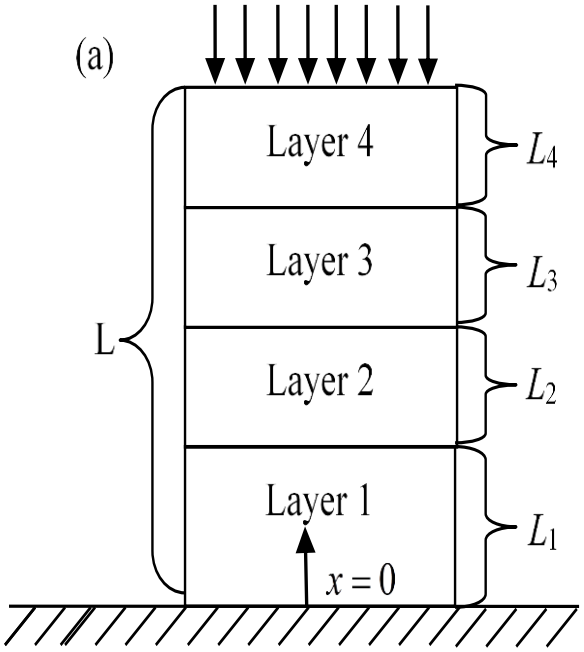

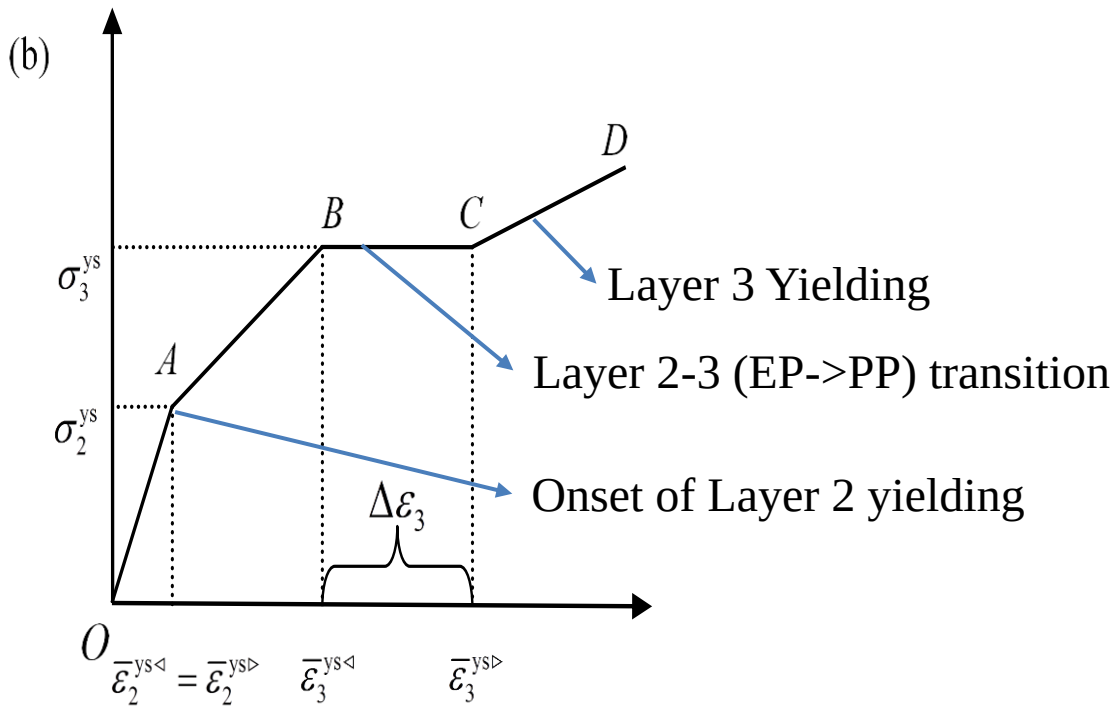

Plastic Potential $$V_i(\varepsilon_i^{\mathrm{p}}, \varepsilon_{i,x}^{\mathrm{p}}) = \sigma_i^{\mathrm{ys}} \left|\varepsilon_i^{\mathrm{p}}\right| + \frac{1}{2}\beta_i \left[\left(\varepsilon_i^{\mathrm{p}}\right)^2 + \ell_i^2 \left(\varepsilon_{i,x}^{\mathrm{p}}\right)^2\right],$$

Strain Burst $\Delta\varepsilon_3 = \bar{\varepsilon}_3^{\mathrm{ys}\triangleright} - \bar{\varepsilon}_3^{\mathrm{ys}\triangleleft}$

$$= \frac{\left[\ell_2 \mathrm{Sinh}\left(\ell_2^*/2\right)\mathrm{Cosh}\left(\ell_3^*/2\right) + \ell_3 \mathrm{Sinh}\left(\ell_3^*/2\right)\mathrm{Cosh}\left(\ell_2^*/2\right)\right]}{L\left[\beta_2\ell_2 \mathrm{Cosh}\left(\ell_2^*\right)\mathrm{Sinh}\left(\ell_3^*\right) + \beta_3\ell_3 \mathrm{Cosh}\left(\ell_3^*\right)\mathrm{Sinh}\left(\ell_2^*\right)\right]}$$

$$\times 4\ell_2 \mathrm{Tanh}\left(\ell_2^*/2\right)\mathrm{Sinh}\left(\ell_2^*/2\right)\mathrm{Sinh}\left(\ell_3^*/2\right)\left(\sigma_3^{\mathrm{ys}} - \sigma_2^{\mathrm{ys}}\right).$$

$\ell_i^* = L_i / \ell_i$

Fitting Model to Experiment

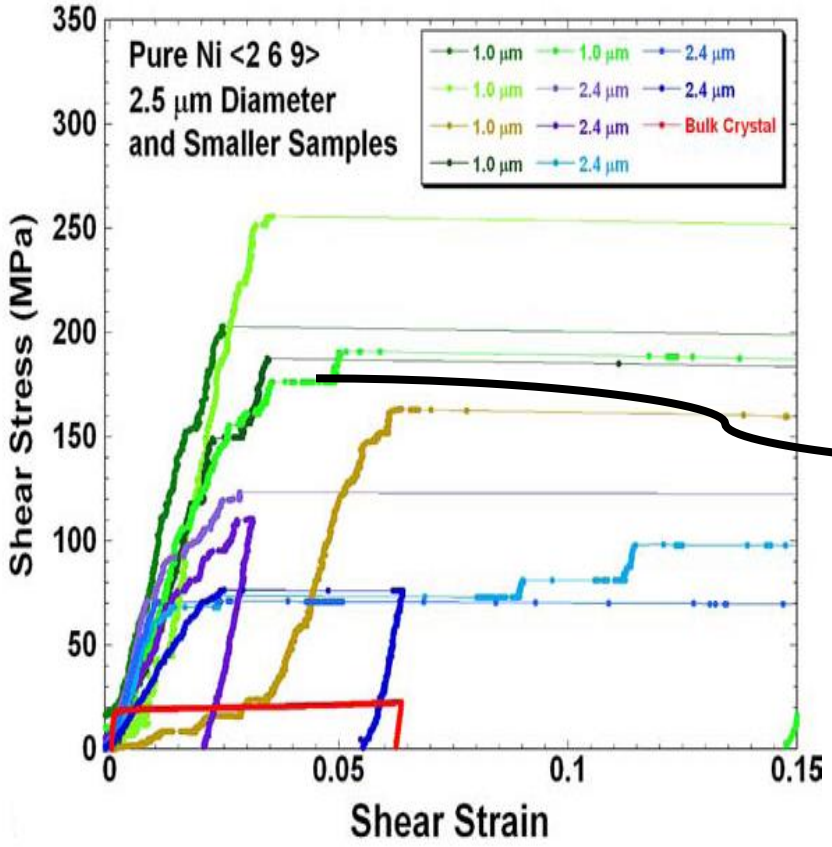

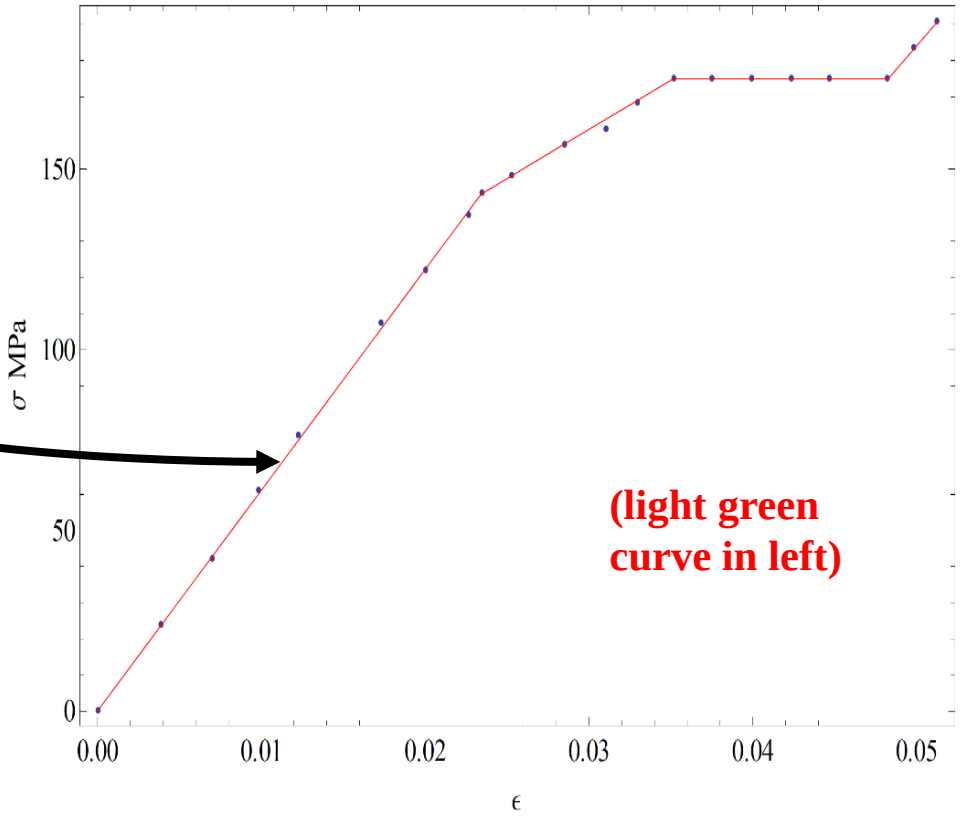

(light green curve in left)

Shear modulus G (GPa)	Yield stress (MPa)		Layer thickness (μm)	Inner length scale (μm)
	σ_2^{ys}	σ_3^{ys}	$L_1 = L_2 = L_3 = L_4$	$\ell_2 = \ell_3$
6.1	143	175	0.625	1.95

	AB (Layer 2 yield)	*BC* (1st strain burst)	*CD* (Layer 3 yield)
β_2 (GPa)	0.138	0.138	5.966
β_3 (GPa)		0.117	5.966

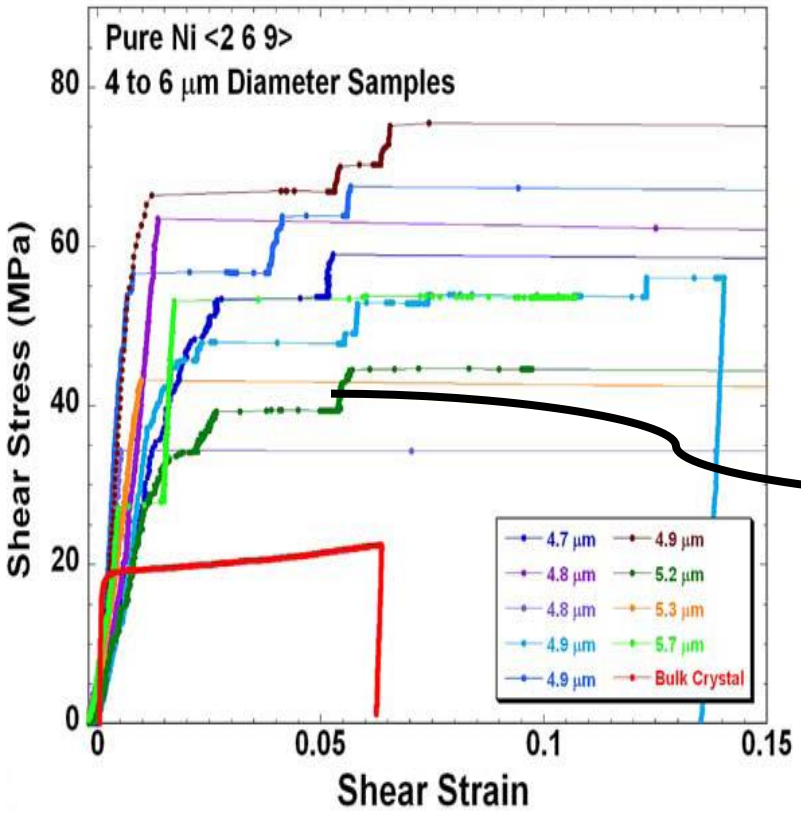

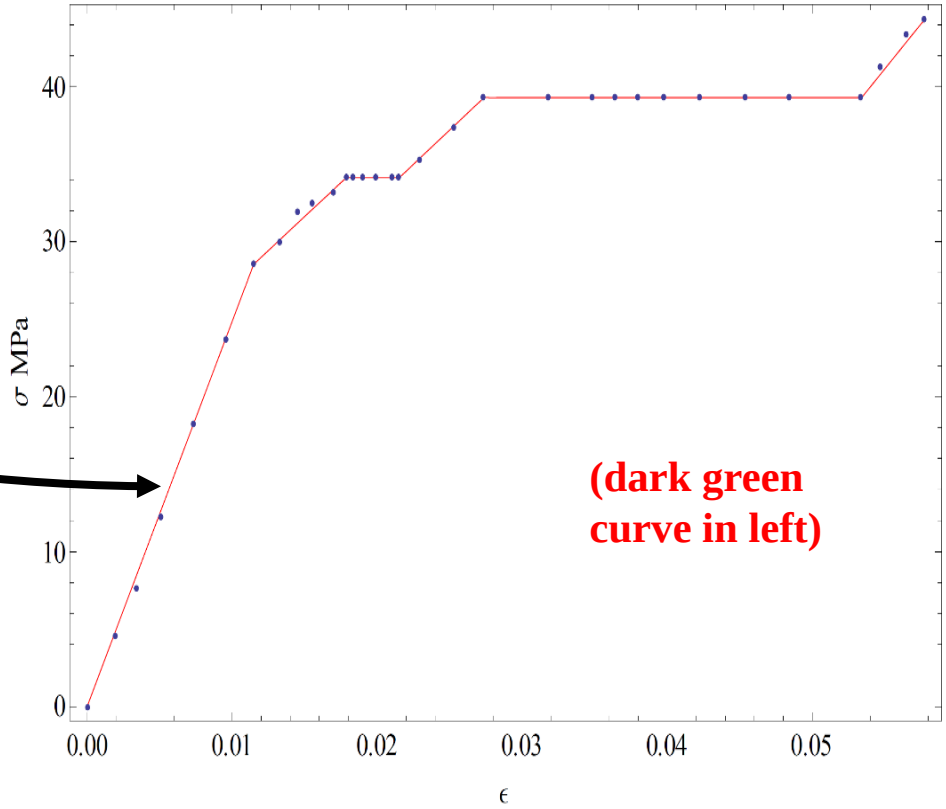

(dark green curve in left)

X. Zhang, K. E. Aifantis, *Mater. Sci. Engng.: A* 528, 5036 (2011).

Parameters used to generate stress–strain plot for 5.2 μm diameter micropillar.

Shear modulus G(GPa)	Yield stress (MPa) σ_2^{ys}	σ_3^{ys}	σ_4^{ys}	Layer thickness $L_1=L_2=L_3=L_4=L_5$ (μm)	Inner length scale $\ell_2=\ell_3$ (μm)
2.485	28	34	39	2.6	1.95

	AB (Layer 2 yield)	BC (1st strain burst)	CD (Layer 3 yield)	DE (2nd strain burst)	EF (Layer 4 yield)
β_2(GPa)	0.034	0.034	0.191	0.021	0.679
β_3(GPa)		0.101	0.191	0.021	0.679
β_4(GPa)				0.021	0.679

Capturing the Upper and Lower Bounds

A five-layers configuration is used to obtain the lower bound, while a four-layers configuration is used to obtain the upper bound.

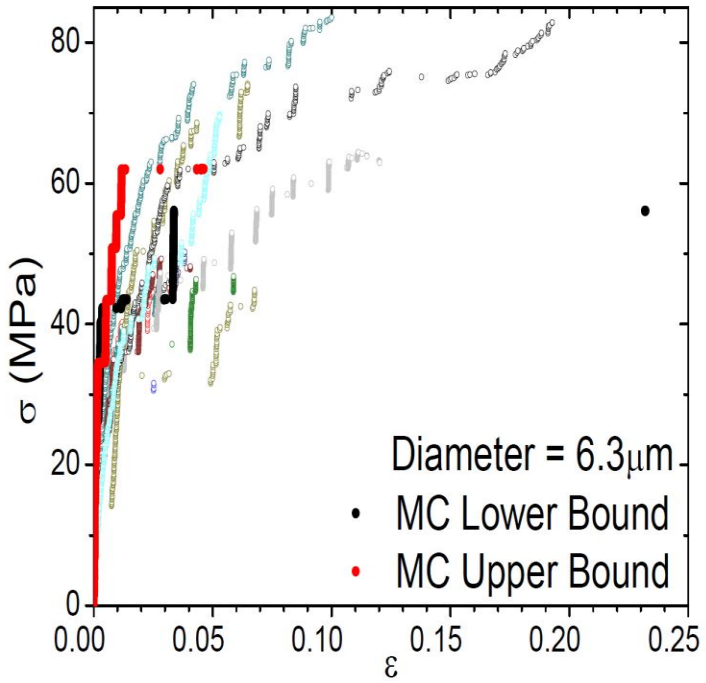

K. S. Ng, A. H. W. Ngan, *Modell Simul Mater Sci Eng* 16, 055004 (2008).

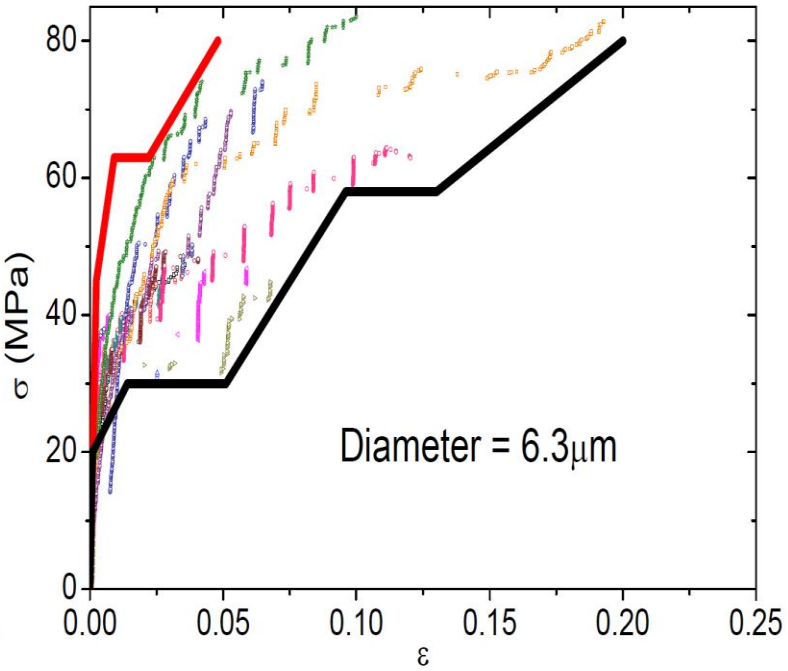

X. Zhang, K. E. Aifantis, A. Ngan, forthcorming

- **The bounds/envelope captured by the strain gradient multilayer model is more consistent than those obtained using MC.**
- **The calculation is not elaborate; more importantly, the deformation mechanism is considered.**

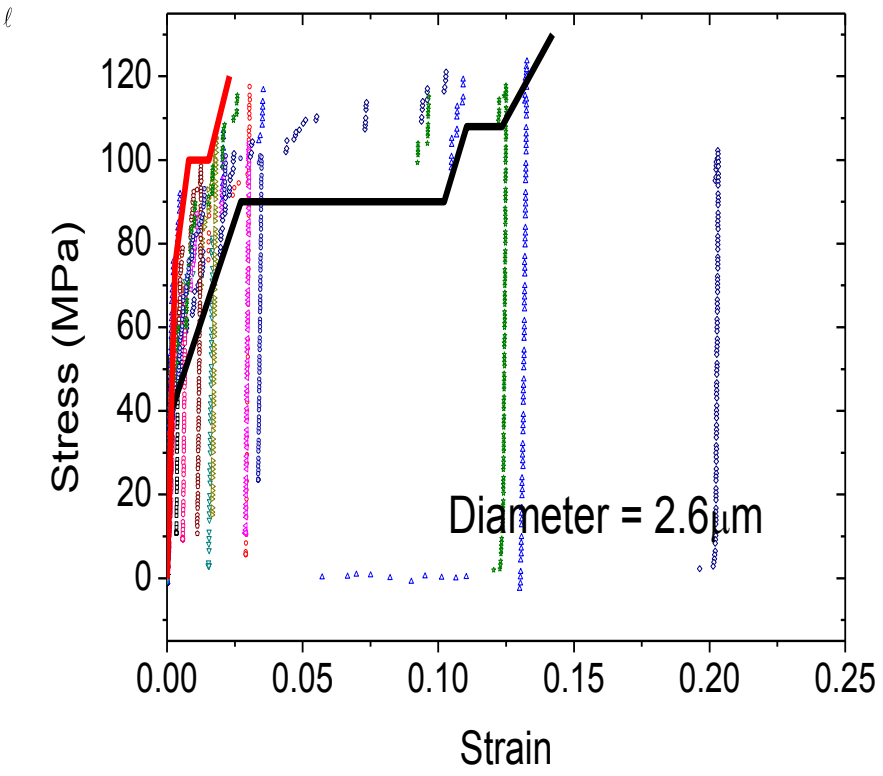

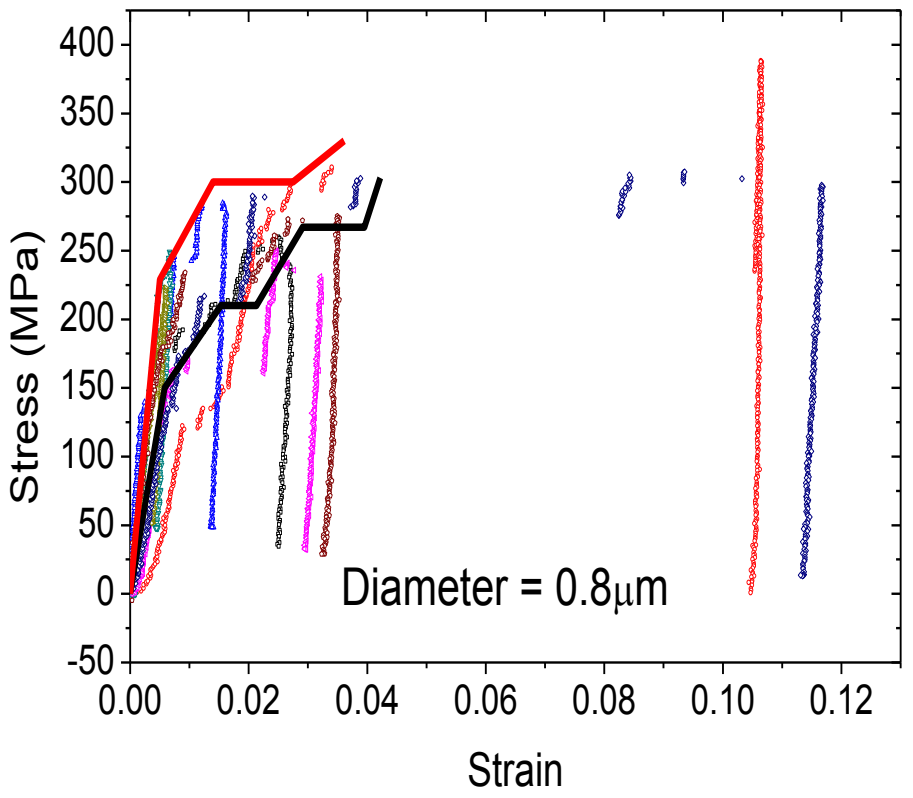

		Two strain bursts lower bound			One strain burst upper bound		
Pillar diameter	L (μm)	6.3	2.6	0.8	6.3	2.6	0.8
Layer thickness	L_i (μm)	5.04	2.08	0.64	6.3	2.6	0.8
Internal length scale	ℓ (μm)	3.5	1.5	0.5	4	2	0.6

*aspect ratio (height/diameter) of the pillar was 4:1

➢**Internal length scale could be related to the layer thickness; since the larger the layer thickness, the larger the internal length.**

Stochasticity & Serrations in Compressed Micropillars

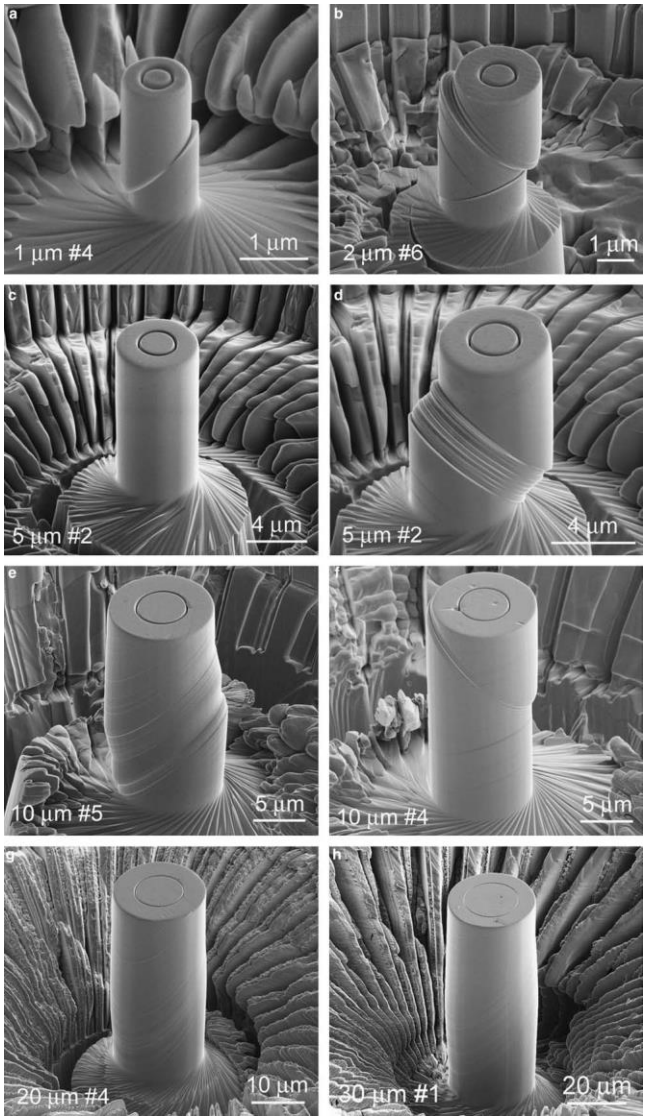

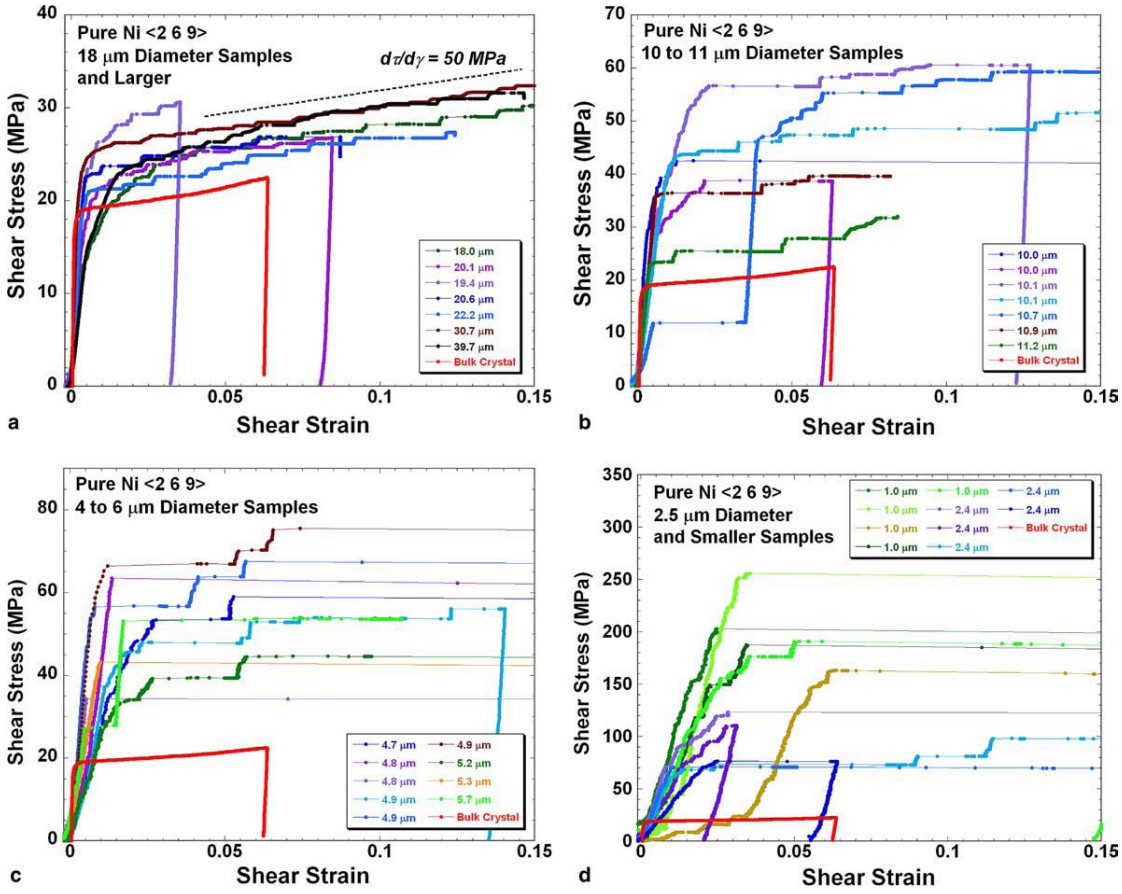

Dimiduk et al, 2005

- ***Serrated Plastic Flow in Micropillars***
  - *Governing Deterministic Equations*

$$\sigma_i = E_i(\varepsilon_i - \varepsilon_i^P),$$

$$\beta_i \varepsilon^P - \beta_i \ell_i^2 \frac{d^2\varepsilon_i^P}{dx^2} = (\sigma_0 - Y_i)$$

(Zhang and K.E. Aifantis, 2011)

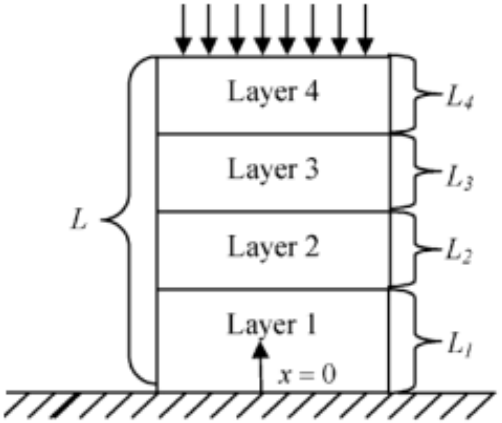

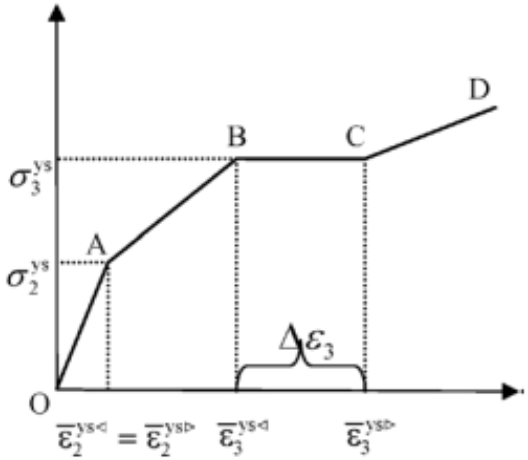

  - *Serrations*

Strain bursts ($\Delta\varepsilon$) are obtained due to the occurrence of discontinuity of the hyperstress $\tau = \beta\ell^2(d^2\varepsilon^P/dx^2)$ between "elastic/no-yielding" and "plastic/yielding" layers

  - *Introducing Stochasticity*

$$Y_i = Y^0 + Y_i^{weib} = (1+\delta)Y^0$$

$$PDF(\delta) = \frac{\kappa}{\lambda}\left(\frac{\delta}{\lambda}\right)^{\kappa-1} e^{-(\delta/\lambda)^\kappa}; \quad \bar{\delta} = \lambda\Gamma\left[1+(1/\kappa)\right], \quad \left\langle\delta^2\right\rangle = \lambda^2\Gamma\left[1+(2/\kappa)\right] - \bar{\delta}^2$$

κ/λ : shape/scale parameters

- ***Cellular Automata Simulations***

  - Lattice of 6d×1 cells of size 0.5 μm× d μm (3:1 height to diameter ratio)
  - Force controlled simulation
  - Weibull distributed cell yield stress

- ***Intermittent Size-dependent Micropillar Plasticity***

$$E = 5\ \text{GPa};\quad \beta = 150\ \text{MPa};\quad \ell = 0.5\ \mu\text{m};\quad Y^0 = 80\ \text{MPa}$$

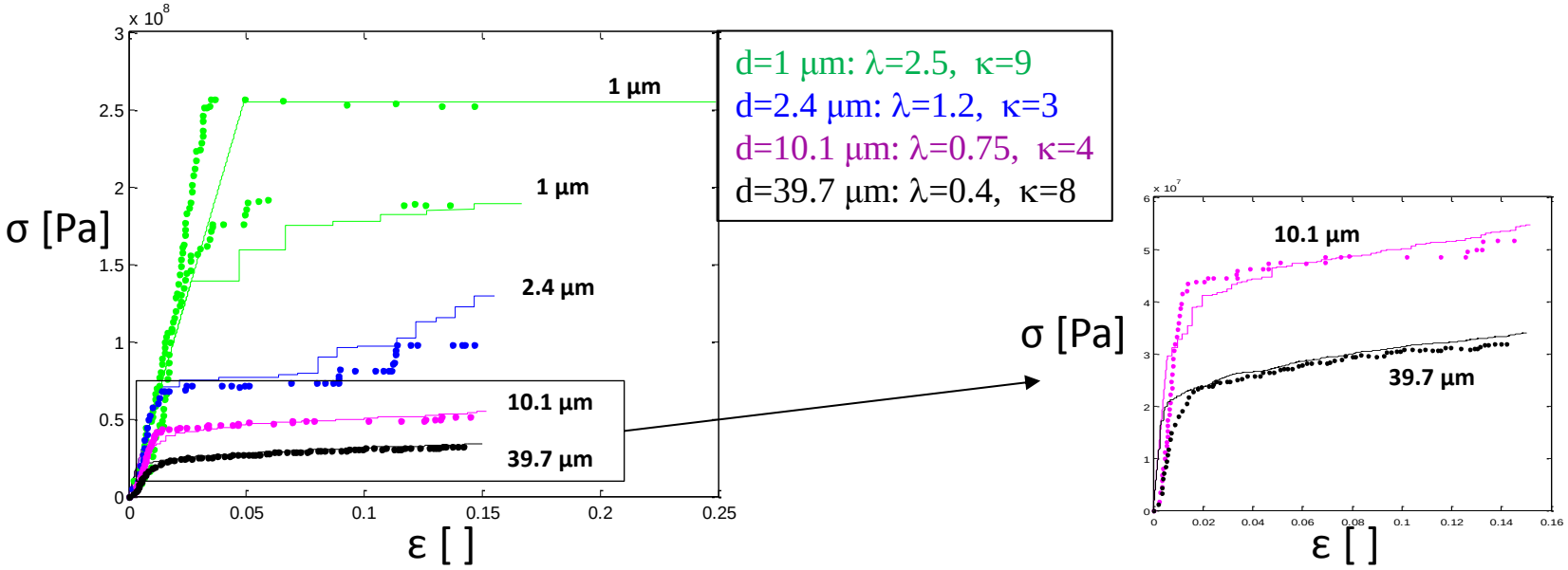

K.E. Aifantis & Konstantinidis, forthcoming

- ***Random Response of Same Diameter (4.9 mm) Micropillars***

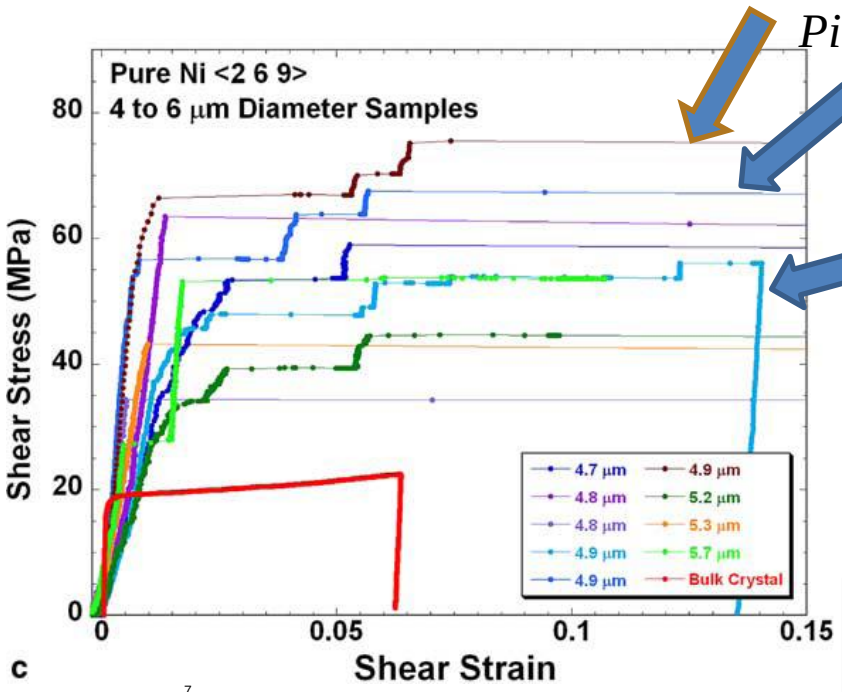

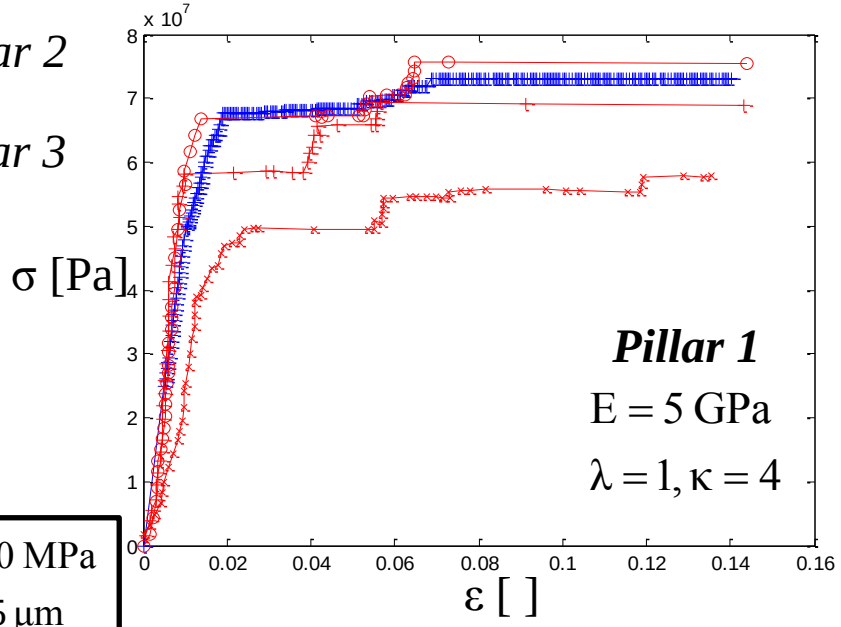

$\beta = 150$ MPa
$\ell = 0.5$ μm
$Y_i^0 = 80$ MPa

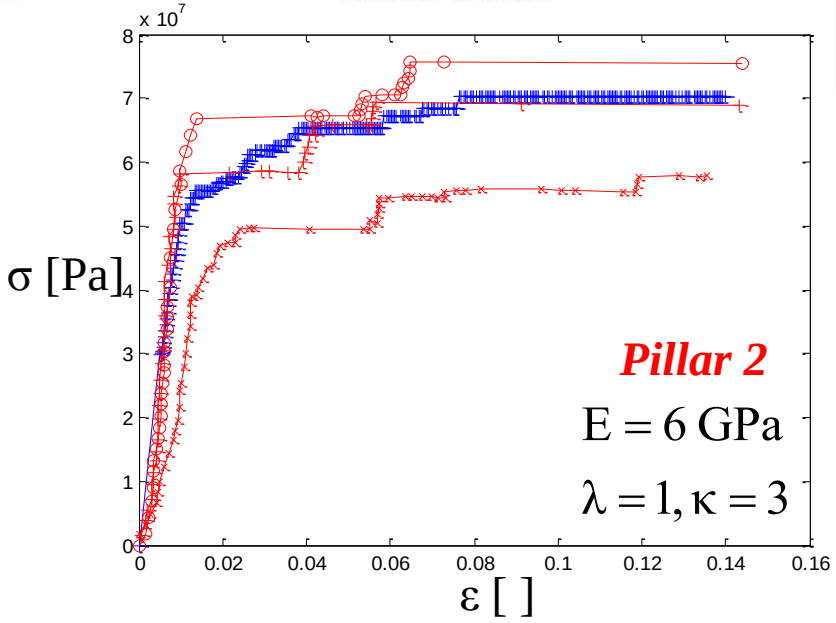

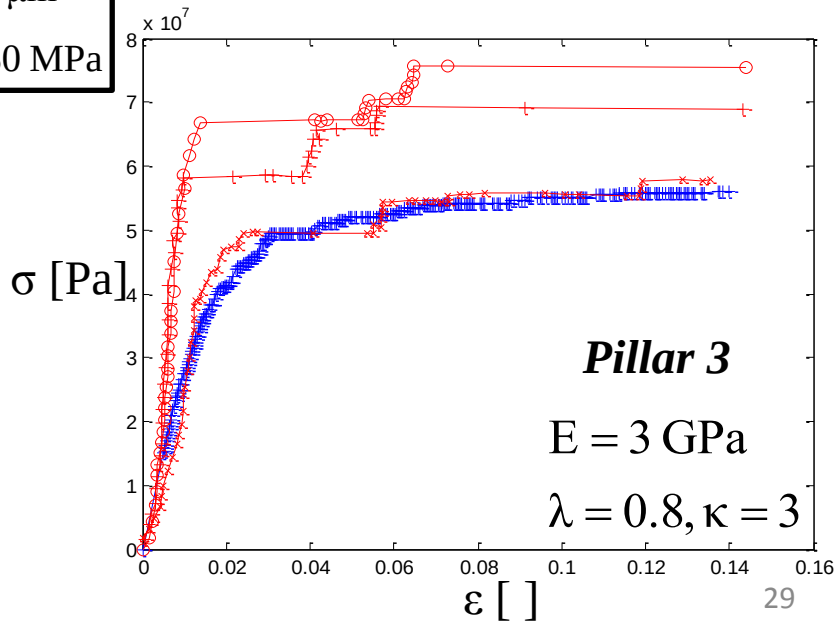

- *Example: Simulation Details for Pillar 2*

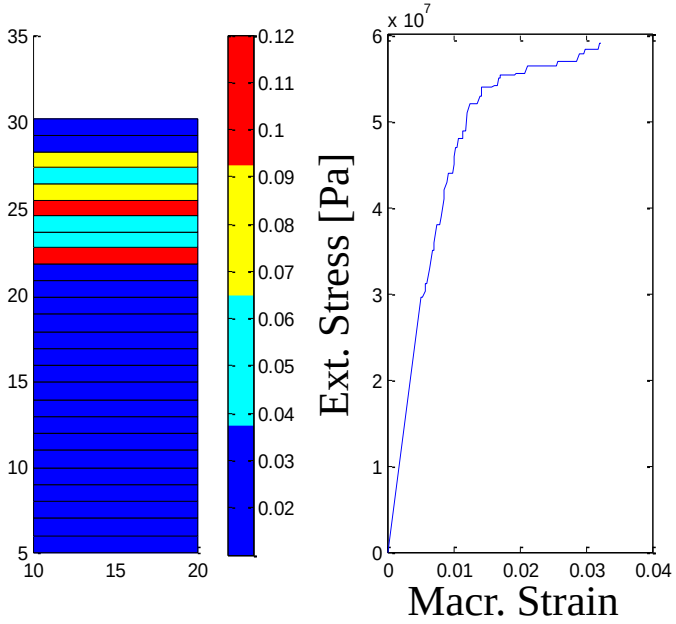

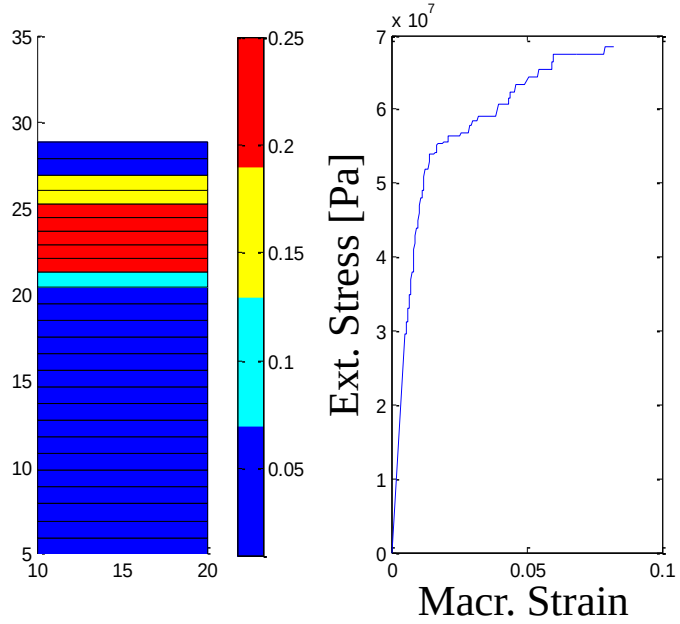

Shear Bands

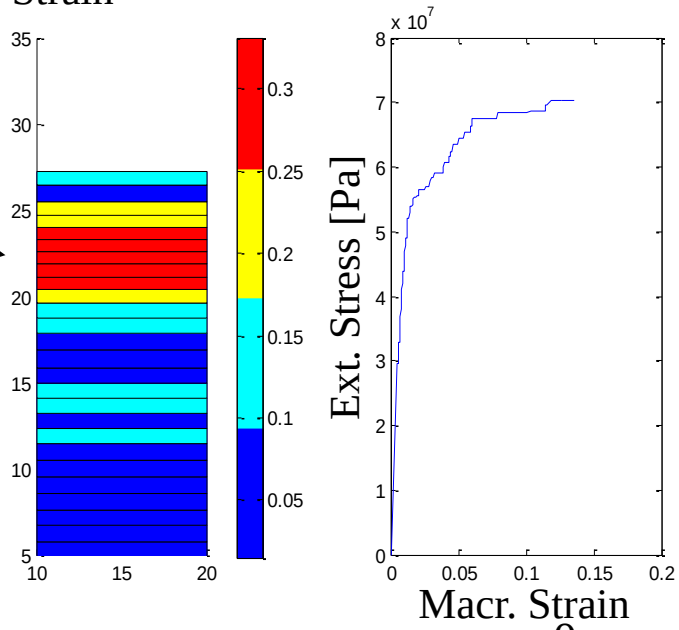

$E = 6\,\text{GPa}; \quad \beta = 150\,\text{MPa}; \quad \ell = 0.5\,\mu\text{m}; \quad Y_i^0 = 80\,\text{MPa}; \quad \lambda = 1, \kappa = 3$

II. MECHANICAL RESPONSE OF TRICRYSTALS

Tension Behavior of Tricrystal through DDD Simulation

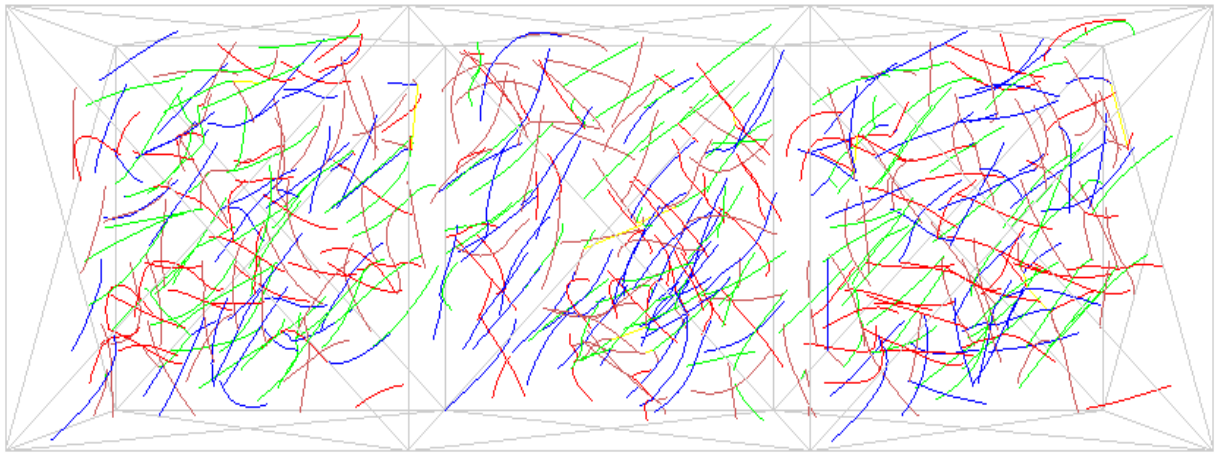

Grain size: 750 nm

Loading axis : [001] axis of all grains

Misorentation of grain boundary: 157.5°

Dislocation source length: 100nm 200nm, 300nm

Initial dislocation density: $3.75\times10^{13}\mathrm{m}^{-2}, 7.5\times10^{13}\mathrm{m}^{-2}, 10.25\times10^{13}\mathrm{m}^{-2}$

Strain rate: 5000/s

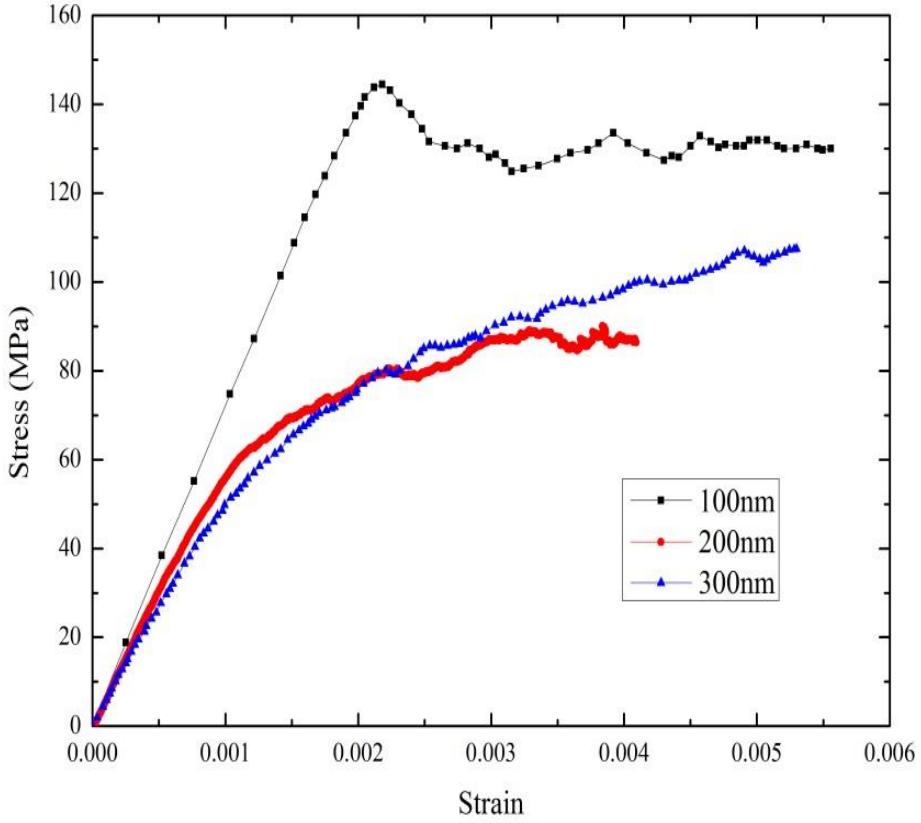

Dislocation source length (nm)	100	200	300
Yield stress (MPa)	114	65	43
Elastic modulus (GPa)	72	60	53

The higher the dislocation source length, the lower the yield stress and elastic modulus

$$\alpha_{ij}(x) = \left\langle \frac{1}{\Delta V(x)} \sum_{x_i \in \Delta V(x)} l_i \otimes b_i \right\rangle$$

α_{32}

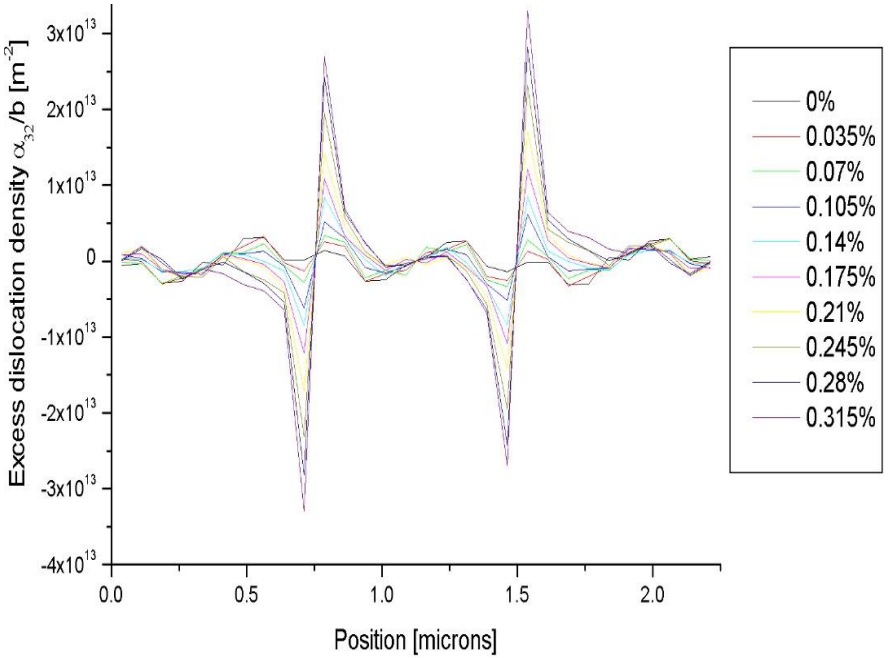

$$\alpha_{\text{in}} = e_{nkj}\gamma_{ij,k} \quad \varepsilon_{ij}^{\text{p}} = \left(\gamma_{ij} + \gamma_{ji}\right)/2$$

$\alpha_{32} \Rightarrow \varepsilon_{11}^{\text{p}}$

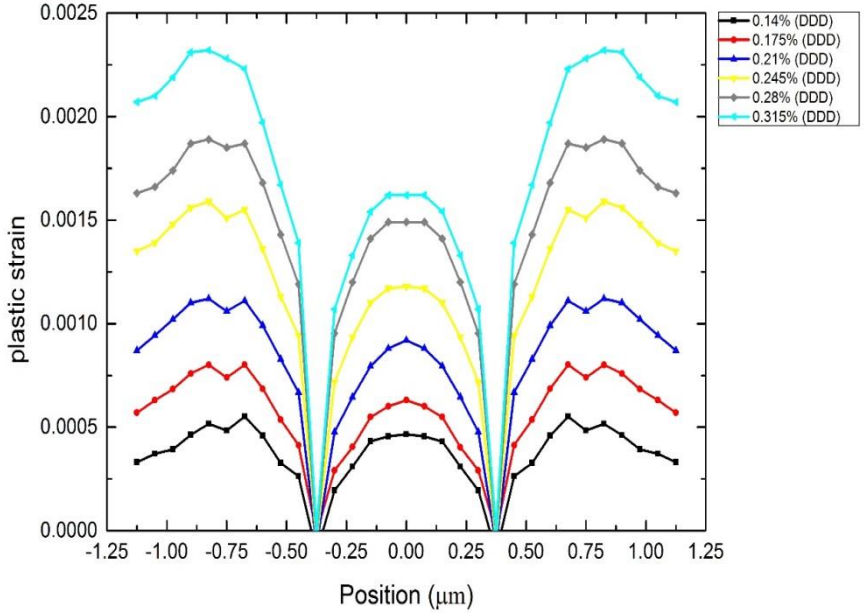

The distribution and evolution of GND density a_{32} during the deformation until strain level of 0.315% for tricrystal with dislocation source length of 200 nm.

Plastic strain profile of tricrystal with dislocation source length of 200 nm

Tension Behavior of Tricrystal through Strain Gradient Theory

Field equation

$$\frac{d^2\varepsilon_i^{\mathrm{p}}}{dx^2}-\frac{\varepsilon_i^{\mathrm{p}}}{\ell_i^2}+\frac{\bar{\sigma}-\sigma_i^{\mathrm{ys}}}{\beta_i\ell_i^2}=0 \qquad \frac{du_i}{dx}-\varepsilon_i^{\mathrm{p}}-\frac{\bar{\sigma}}{E_i}=0$$

Boundary condition

$$\varepsilon_{\mathrm{L}}^{\mathrm{p}}(-\frac{1}{2}L)=\varepsilon_{\mathrm{M}}^{\mathrm{p}}(-\frac{1}{2}L)=0 \qquad u_{\mathrm{L}}(-\frac{3}{2}L)=0,$$

$$\varepsilon_{\mathrm{R}}^{\mathrm{p}}(\frac{1}{2}L)=\varepsilon_{\mathrm{M}}^{\mathrm{p}}(\frac{1}{2}L)=0 \qquad u_{\mathrm{L}}(-\frac{1}{2}L)=u_{\mathrm{M}}(-\frac{1}{2}L),\quad u_{\mathrm{R}}(\frac{1}{2}L)=u_{\mathrm{M}}(\frac{1}{2}L),$$

$$\tau_{\mathrm{L}}(-\frac{3}{2}L)=\tau_{\mathrm{R}}(\frac{3}{2}L)=\gamma_{\mathrm{sf}} \qquad u_{\mathrm{R}}(\frac{3}{2}L)=3L\varepsilon.$$

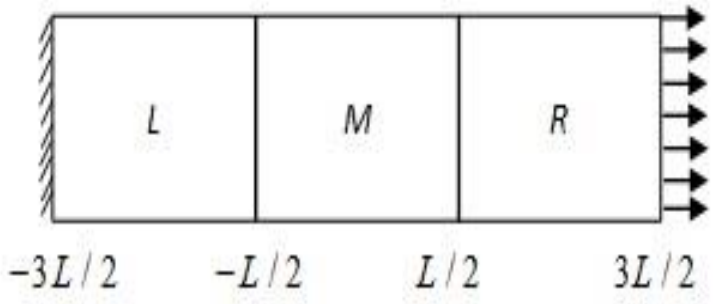

Rigid Grain Boundary

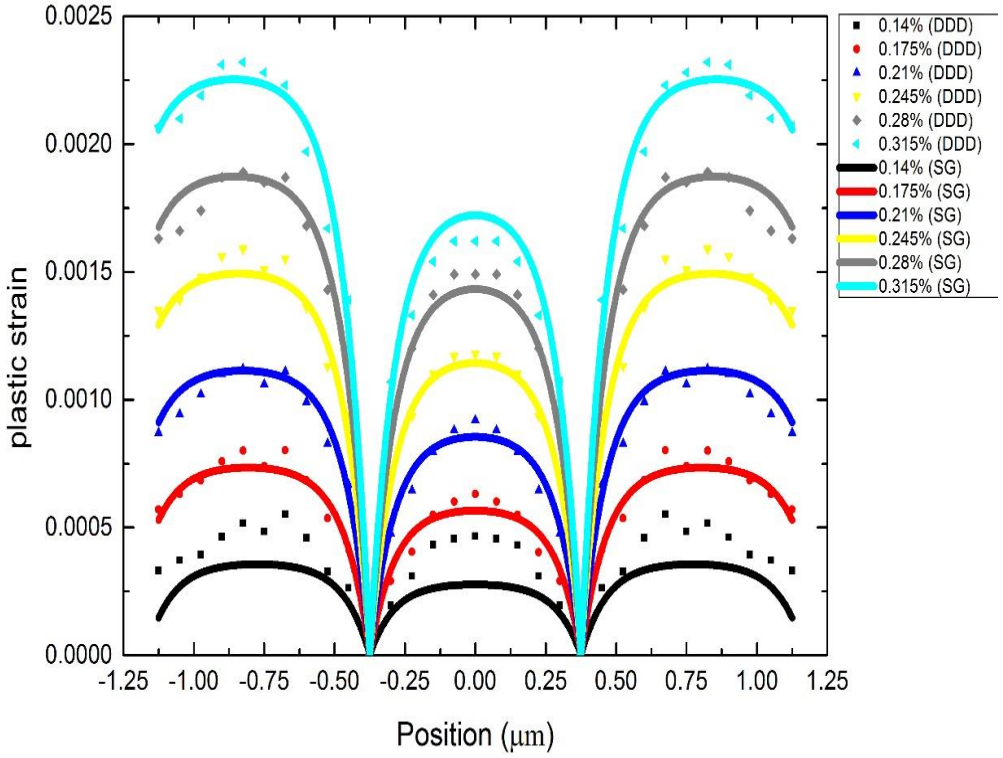

SG fitting for the plastic strain profile of tricrystal with dislocation source length of 200 nm and rigid grain boundary

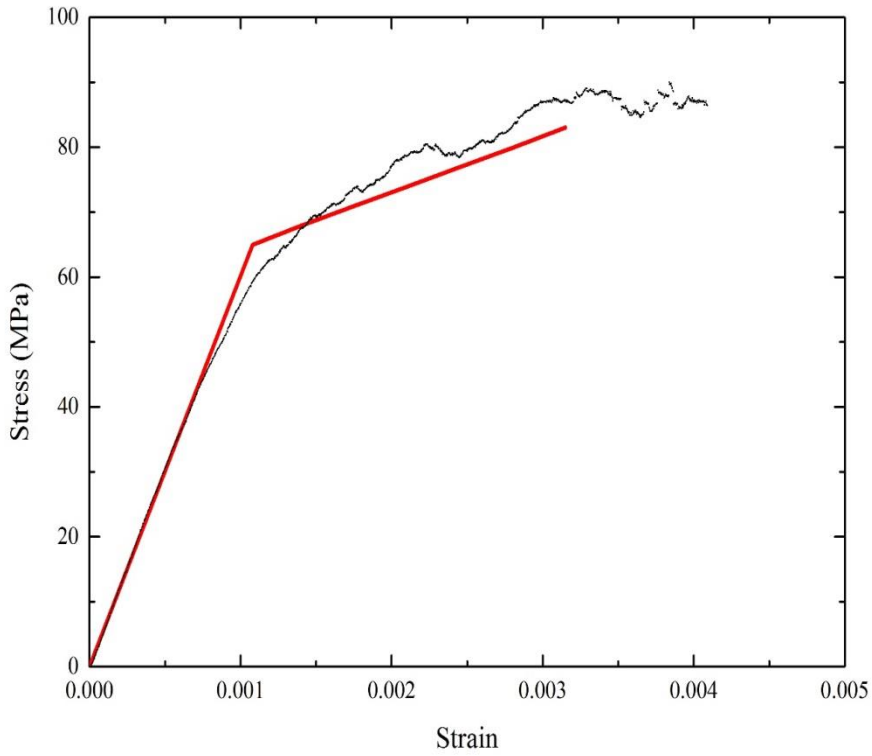

Comparison between the stress-strain curve obtained from DDD and SG theory for tri-crystalline with dislocation source length of 200 nm and rigid grain boundary

Penetrable Grain Boundary

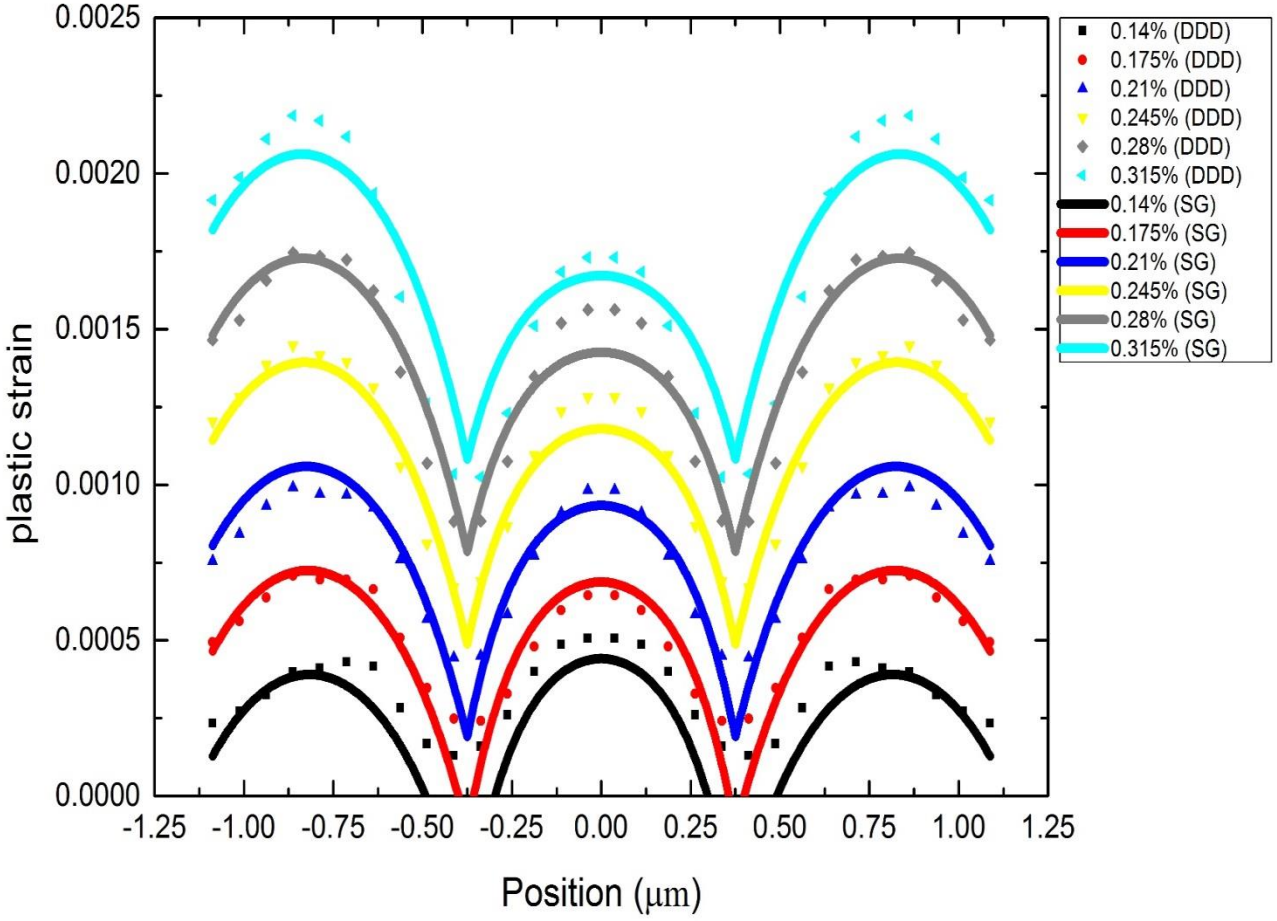

SG fitting for the plastic strain profile of tricrystal with dislocation source length of 200 nm and penetrable grain boundary

III. CHEMOMECHANICAL RESPONSE OF LIBs

KEA et al (2003) + Book (2010)

- ***Chemomechanics*** $\begin{cases} \textit{Anodes (-)} : & Li C_6 \rightarrow Li^+ + e^- + C_6 \\ \textit{Cathodes (+)} : & Li^+ + e^- + MO_2 \rightarrow LiMO_2 \end{cases}$

- ***Anodes / Experimental Observations***

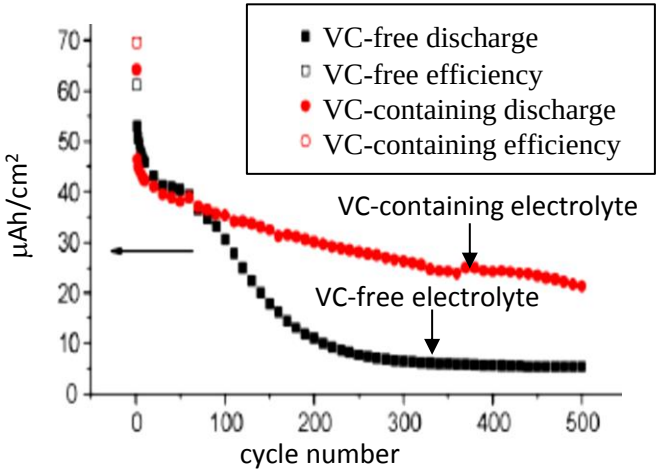

Si thin films cycled in a VC-free and VC-containing electrolyte

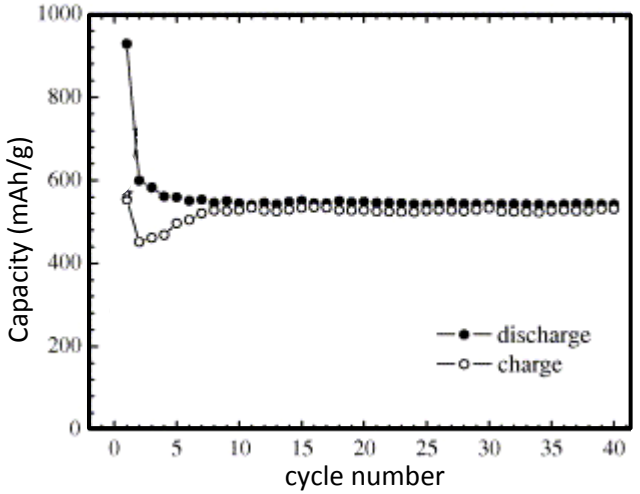

Capacity retention of SnS/C nanocomposite thin film

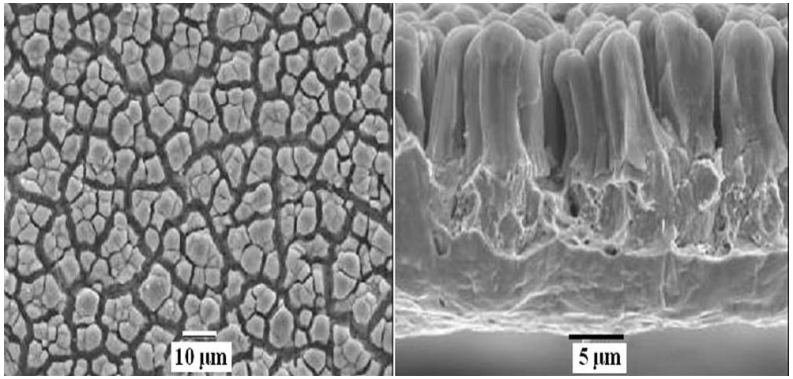

SEM images of 6mm Si film anode after 250 cycles (gave capacities of 1.8mAh/cm²), **(a)** surface, **(b)** cross section. It can be seen that Li-insertion and de-insertion in the first cycles resulted in Si-micron fibres/columns

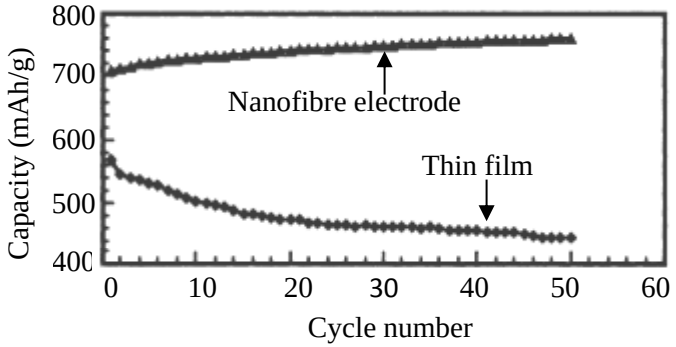

Comparison of capacity retention between SnO_2 nanofibre and SnO_2 thin film electrodes, at a charge/discharge rate of 8C over the potential window of 0.2-0.9V

• *Linear Fracture Mechanics*

- *Effect of Volume Fraction*

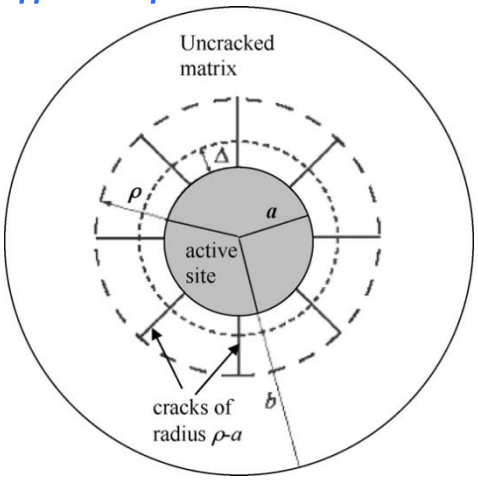

Configuration of unit cell used in analysis; a and b are the radii of the active site and matrix, is the free expansion of the active site if it were not constrained (by the matrix), and is the crack radius

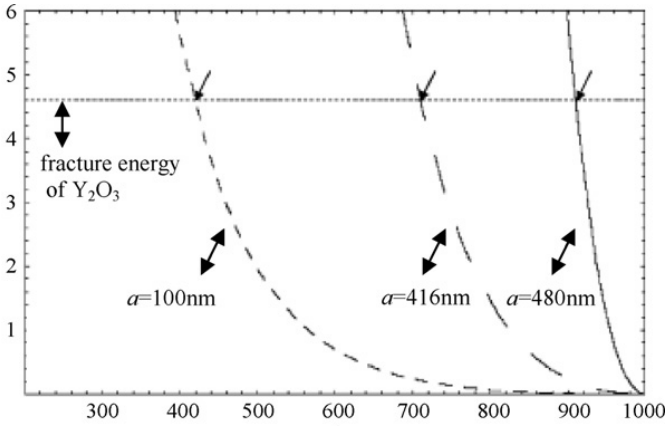

Griffith's criterion for various volume fractions (b is kept 1000m), of Si nanospheres (with radius a) embedded in a Y_2O_3 matrix. Arrows indicate the crack radius at which fracture will stop

- *Effect of Aspect Ratio*

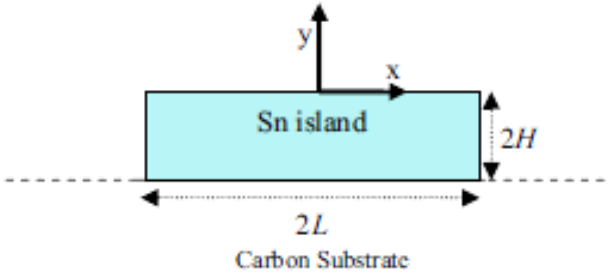

Schematical representation of Sn/C island microstructure

$$\frac{H}{L} \rangle 0.3$$

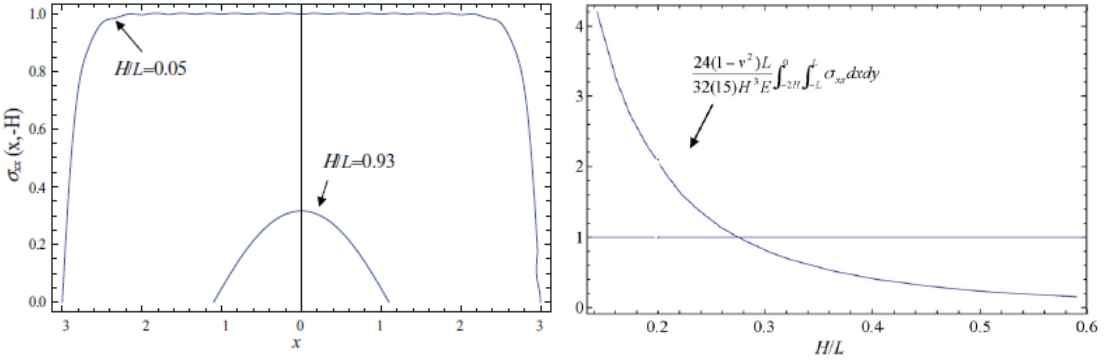

(a) **(b)**

(a) Comparing the normalized compressive stress for different H/L values. **(b)** In order for the islands to remain attached to the carbon, their height/length ratio (*H/L*) must be greater than 0.3

• *Gradient Damage Mechanics*

- *Effect of the Interplay of Particle Size and Interparticle Spacing*

$$\Pi = \Pi_{\text{int}} - \Pi_{ext} = \int_{\Omega} \tilde{\psi}\left(\boldsymbol{\varepsilon}, d, \varphi_d, \nabla\varphi_d\right) dV - \int_{\partial\Omega_\sigma} \boldsymbol{u}\cdot\boldsymbol{t}\, dA$$

$$\tilde{\psi} = \frac{1}{2} f(d)(\varepsilon : C : \varepsilon) + g(d) + \frac{c_d}{2}\|\nabla\varphi_d\|^2 + \frac{\beta_d}{2}\left[\varphi_d - H_\varphi(d)\right]^2$$

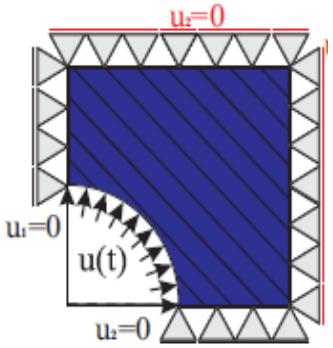

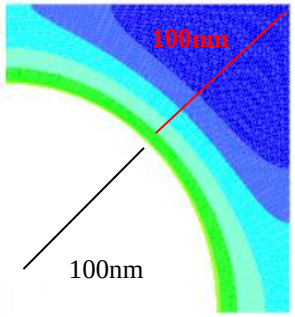

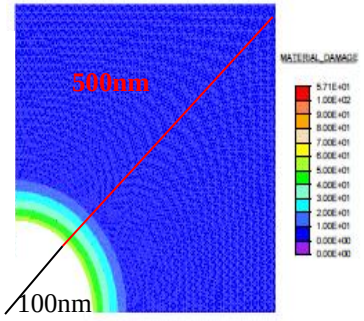

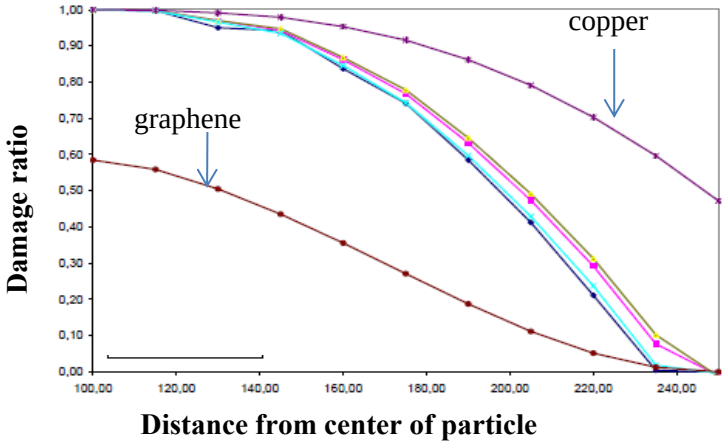

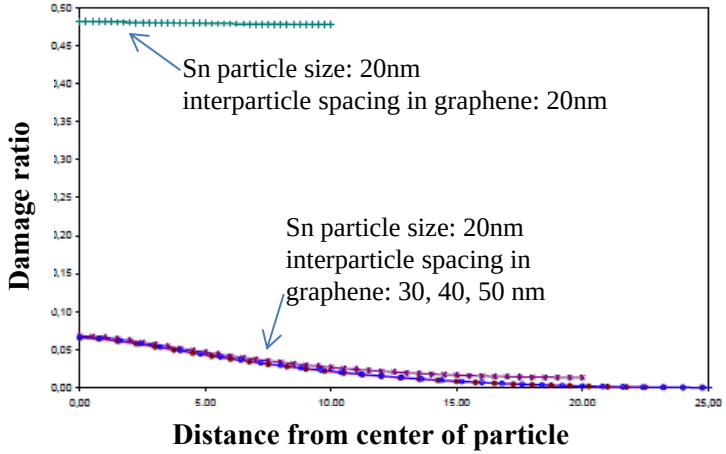

It is predicted that graphene is the most promising matrix material since it results for the least damage, while Cu results in the greatest damage. This is according to experimental.

It is predicted that damage is minimal when the interparticle spacing is 1.5 times greater than the particle size.

• *Cathodes / Experimental Observations*

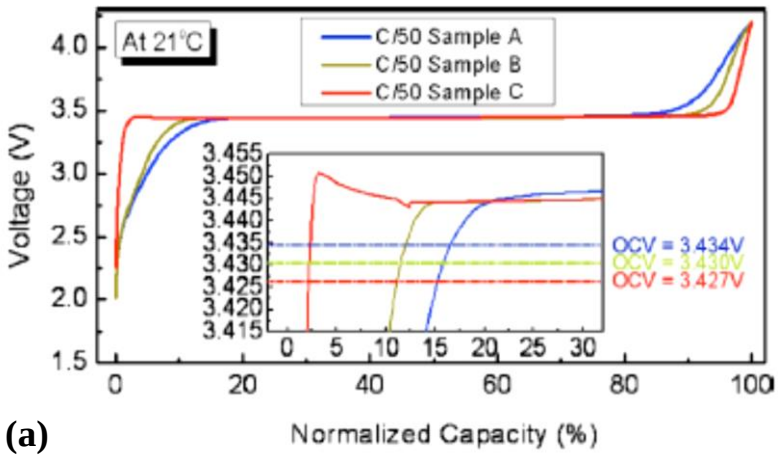

(a)

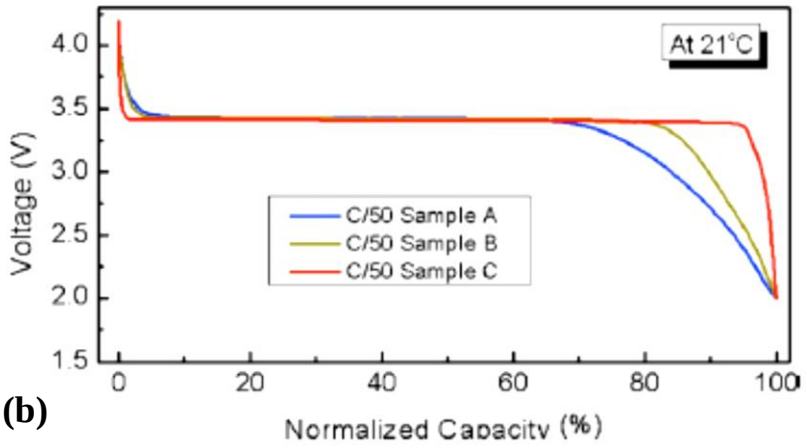

(b)

Galvanostatic charging **(a)** and discharging **(b)** at C/50 rate for LiFePO4 shows the narrower composition range over which smaller size particles exhibit a constant cell voltage corresponding to two-phase coexistence

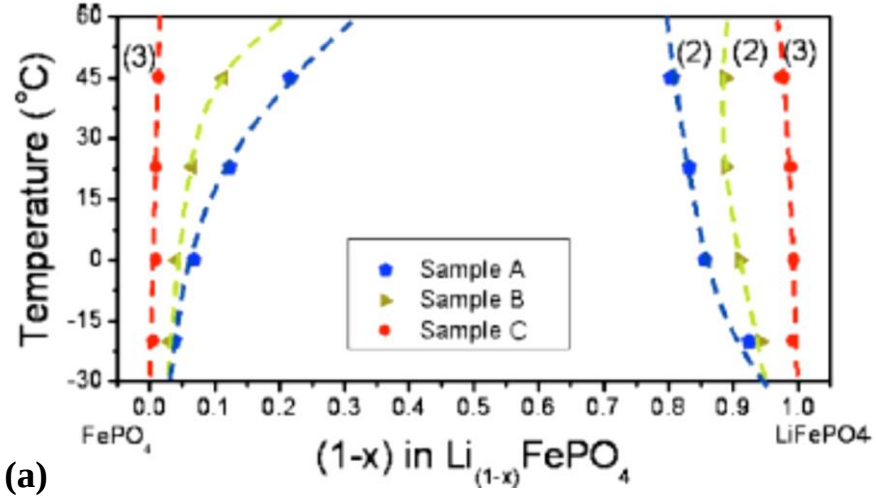

(a)

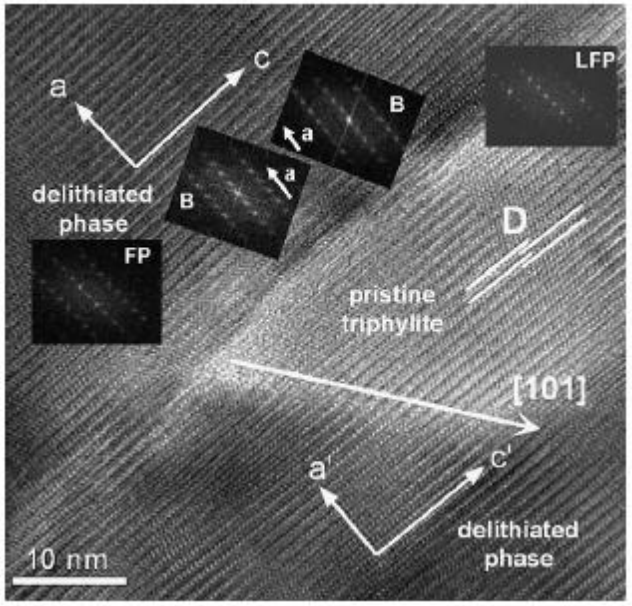

(b)

(a) Experimentally determined phase diagram for nanoscale lithium iron phosphate as a function of particle size. It is observed that the miscibility gap contracts systematically and solid solution limits increase with decreasing particle size and increasing temperature. **(b)** HRTEM image of the 0.5(LiFePO4 + FePO4) sample showing a LiFePO4 cluster in the *ac*-plane. Inserts are the fast Fourier Transform of the selected regions, namely LiFePO4 (LFP) domain, FePO4 (FP) domain and across the boundary (B). The splitting of spots of diffraction maxima along *a*-direction due to a compositional difference along with lattice parameters (see text) is evident in the FFTs represented as "B" (for boundary)

• *Chemomechanical Models*

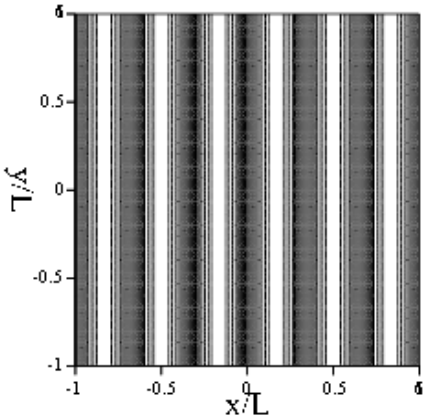

Periodic variation in composition (gray scale) along the *x* direction in a crystal having a half thickness of L

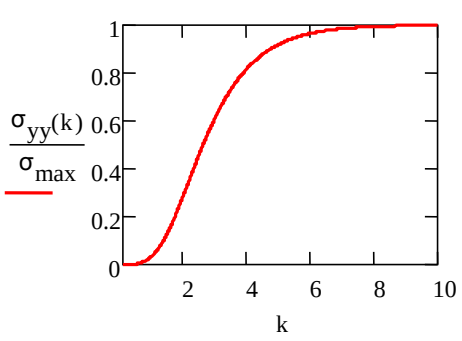

Correlation between primary stress component at the crystal center (y=0) and $\boldsymbol{k}=n\pi$

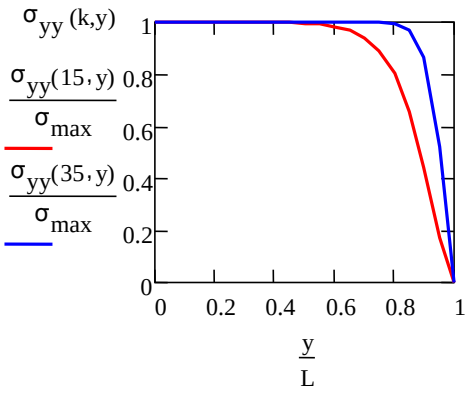

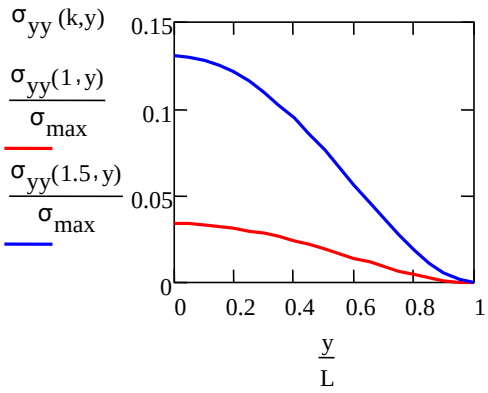

Distribution of principle stress magnitude across the crystal as a function of k

$$c = \varepsilon \sin\left(n\pi \frac{x}{L}\right) + c_0$$

$$\sigma_{yy} = -\sin\left(\frac{k}{L}x\right) A\cosh\left(\frac{k}{L}y\right)\left(\frac{k}{L}\right)^2 + \sin\left(\frac{k}{L}x\right) E\alpha\varepsilon\nu - \sin\left(\frac{k}{L}x\right) Dy\sinh\left(\frac{k}{L}y\right)\left(\frac{k}{L}\right)^2$$

$$\frac{d^2}{dx^2}G_h + 2\frac{E}{1-\nu}a^2\left[-1\frac{\sinh(k)+1\cosh(k)k}{1(\cosh(k)\sinh(k)+k)}+1\right]^2 + 2\kappa\left(\frac{k}{L}\right)^2 < 0$$

$$L_{cr} = \left[(1-\nu) - 4935\kappa\left[\frac{d^2}{dx^2}G_h(1-\nu)250 + 211E\alpha^2\right]^{-1}\right]^{1/2}$$